Lindblad driving for nonequilibrium steady-state transport for noninteracting quantum impurity models

Matthias Bauer

München 2011

Lindblad driving for nonequilibrium steady-state transport for noninteracting quantum impurity models

Matthias Bauer

Bachelorarbeit
an der Fakultät für Physik
der Ludwig–Maximilians–Universität
München

vorgelegt von
Matthias Bauer
aus Baden-Baden

München, den 26. Juli 2011

Gutachter: Prof. Dr. Jan von Delft

Contents

Abstract

In this Bachelor thesis we provide a first consistency check for a Lindblad approach in the context of nonequilibrium transport in quantum impurity models with local interactions. To this end we discuss the derivation and steady-state properties of quantum master equations (QME) in Lindblad form for different noninteracting fermionic toy-models. In particular, we investigate the transport properties of the considered systems. These range from a simple resonant level with Lindblad drive to a central level coupled to two explicitly modeled leads of up to 140 modes each of which is stabilized by its respective Lindblad baths.

Starting with an iterated Liouville-von Neumann equation for the reduced density matrix of the system we find that a Born-Markov approximation yields a QME in Lindblad form that describes the steady-state properties of the resonant level model properly. For two levels this approximation is found to be still valid whereas we do not directly obtain a Lindblad QME.

Therefore, we consider two different approximation schemes. It was found that a derivation in the eigenbasis of the Hamiltonian requires a secular approximation in order to arrive at a Lindblad QME. This can be understood as an effective averaging over the intersubsystem coupling and we always find a vanishing particle current for this approach. However, occupation numbers are reproduced correctly in equilibrium. Introducing a local approximation we obtain a different Lindblad QME with separate contributions for each level plus bath subsystem in the dissipator. For this approach we find a finite current which qualitatively agrees with the Keldysh results in a certain parameter regime. Furthermore we show that for a simple Aharanov-Bohm geometry phase coherence of the steady-state current is preserved.

In the end we consider a central level coupled to two leads with explicitly modeled modes in the local approximation. We numerically investigate the transport properties of this model for up to 140 lead modes and find an excellent agreement with the Keldysh results in the wide-band limit and the regime of strong intersubsystem coupling.

1. Introduction

The standard tool for describing nonequilibrium steady-state transport through a quantum system coupled to two leads with different chemical potentials is the Keldysh formalism [1]. However, when the quantum system is interacting, the treatment of interactions within the Keldysh formalism is difficult: a perturbative expansion is inadequate for some applications (e.g. involving the Kondo effect), and numerical treatments of the interaction in the Keldysh formalism are very cumbersome.

Therefore, it is of interest to explore theoretical frameworks other than the Keldysh approach for dealing with nonequilibrium steady-state transport. One possibility is to use a Liouville equation with Lindblad driving terms that are designed to stabilize the nonequilibrium occupations of the states in the two leads. Such an approach has potential for describing nonequilibrium steady-state transport in the context of quantum impurity models with local interactions [2].

An important consistency check for such a Lindblad approach is that its results should coincide with those of the Keldysh approach. While such a check is, in general, difficult for interacting models, it is also important and relevant for noninteracting ones, where it *can* be performed explicitly.

In this Bachelor thesis we therefore explore the microscopic derivation of Lindblad drives for several different toy-models, all of which are noninteracting. We analyze their basic properties which makes a first comparison to the exact Keldysh results possible. The promising results might lead the way towards an application of Lindblad drives in more complicated interacting systems.

This thesis is organized as follows.

In a first theoretical part we give a short general introduction to open quantum systems and turn to their description by means of Markovian quantum master equations (QME). These give rise to the so-called Lindblad form of QME and we state their most important properties. Their microscopic derivation is outlined and the necessary approximations are introduced.

After this we consider specific models and derive the Lindblad QMEs describing their dynamics. First we discuss the simplest case of just one level coupled to a Lindblad bath. We then consider the cases of two lead levels coupled to each other or to a small system. Where applicable we compare the results for the current between the lead modes to the exact expression. Furthermore we explore whether phase coherence is preserved for an Aharanov-Bohm like geometry. Having discussed these simple examples we turn to the more complicated case of a single level coupled to up to 140

explicitly modeled lead levels each of which is coupled to its respective Lindblad bath. We derive implicit expressions for the occupations and tunneling terms in the steady state and compare the current through the single level with the exact result.

More explicit calculations and derivations as well as a description of the numerical implementation can be found in the Appendix which will frequently be referred to.

2. Prerequisites

In this chapter we shall restate some of the basic results of quantum mechanics for closed quantum systems in order to compare them to the open system approach outlined in the next chapter. The fermionic operators which will be used to describe our models are introduced. As this is standard textbook material we shall closely follow [3, 4, 5] in both, content and notation. We also use this chapter to establish the notation used throughout this thesis.

2.1. Unitary Evolution of Closed Quantum Systems

Following [4] we denote by a *closed* quantum system a system that is closed in the sense that it does not interchange any information with another system (i.e. energy, particles, etc.). We reserve the term *isolated* to closed systems whose Hamiltonian is time independent[1]. We will work in units of $\hbar = 1$.

The time evolution of a pure state $|\psi(t)\rangle \in \mathcal{H}$ generated by the Hamiltonian $H(t)$ is determined by the Schrödinger equation (2.1):

$$\frac{d}{dt}|\psi(t)\rangle = -iH(t)|\psi(t)\rangle\,, \tag{2.1}$$

whereas the time evolution of a mixed state $\rho(t) \in \mathcal{O}_1(\mathcal{H})$[2] is determined by the Liouville-von Neumann equation (2.2):

$$\frac{d}{dt}\rho(t) = -i\left[H(t), \rho(t)\right]. \tag{2.2}$$

Due to the linearity of the Schrödinger equation its solution is given by an evolution family $U(t, t_0)$ such that

$$|\psi(t)\rangle = U(t, t_0)|\psi(t_0)\rangle\,, \tag{2.3}$$

where $U(t_0, t_0) = \mathbb{1}$ and $U(t, t_0)$ is a unitary operator.

The time evolution operator is determined by the Hamiltonian of the system in question and can formally be written as

$$U(t, t_0) = \mathcal{T}e^{-i\int_{t_0}^{t} H(\tau)d\tau}, \tag{2.4}$$

[1] An example for a closed but not isolated system is an atom in an external classical electromagnetic field

[2] $\mathcal{O}_1(\mathcal{H}) = \{\rho \in \mathfrak{B}(\mathcal{H}) \text{ s.th. } \mathrm{tr}\rho < \infty\}$ is the space of all trace-class operators in the space of bounded linear operators on $\mathcal{H}$

where $\mathcal{T}$ denotes the time ordering operator. For a time-independent Hamiltonian $H \neq H(t)$ this simplifies to

$$U(t, t_0) = e^{-iH(t-t_0)}. \tag{2.5}$$

The time evolution of the density matrix can similarly be expressed in terms of the same evolution family and is given by:

$$\rho(t) = U(t, t_0)\rho(t_0)U^\dagger(t, t_0) \tag{2.6}$$

This can be expressed in terms of an operator $\mathcal{U}_{t,t_0}$ acting on the space of density matrices [5]:

$$\rho(t) = \mathcal{U}_{t,t_0}\rho(t_0), \tag{2.7}$$

where

$$\mathcal{U}_{t,t_0}[\cdot] = U(t, t_0)[\cdot]U^\dagger(t, t_0). \tag{2.8}$$

Upon deriving equation (2.2) and formally integrating it we arrive at the generator $\mathcal{L}_\tau$ of

$$\mathcal{U}_{t,t_0}[\cdot] = \mathcal{T}e^{\int_{t_0}^{t} \mathcal{L}_\tau d\tau}[\cdot] \tag{2.9}$$

which is also called *Liouvillian* [5]:

$$\mathcal{L}_t[\cdot] = -i\,[H(t), \cdot] \tag{2.10}$$

In the following we will only deal with time-independent generators so that the integral in the exponent simplifies to the difference $t - t_0$. We shall refer to operators such as $\mathcal{L}_\tau$ or $\mathcal{U}_{t,t_0}$ which act upon other operators as *superoperators*.

2.2. Schrödinger, Heisenberg and Interaction Picture

So far we have worked in the *Schrödinger picture* in which the states evolve in time whereas the operators remain constant. As is well known [3] we can also consider the operators to be time-dependent with the state-vectors remaining constant. This formulation of quantum mechanics is called *Heisenberg picture*[3]. When the Hamiltonian of the system can be separated into a free part and an interaction one can introduce a third formulation, the so-called *interaction picture*[4]. We shall briefly introduce these different approaches and quote some basic properties and relations between them in Tab. 2.1 (where $H(t) = H_0 + H_I(t)$).

In our studies we will mostly be concerned with the Schrödinger and the interaction picture. The relation between the density matrix in these pictures can be made more

[3] In the following we shall denote Heisenberg operators by an index H

[4] In the following we shall denote interaction picture operators by a tilde. The index S will – with the exception of this section – denote *system* and not Schrödinger.

Schrödinger picture	Heisenberg picture	Interaction picture
$U(t,t_0) = \mathcal{T} e^{-i\int H d\tau}$	$U(t,t_0) = \mathcal{T} e^{-i\int H d\tau}$	$U_0(t,t_0) = e^{-iH_0(t-t_0)}$
$\lvert\psi_S(t)\rangle = U(t,t_0)\lvert\psi_S(t_0)\rangle$	$\lvert\psi\rangle = \lvert\psi_S(t_0)\rangle$	$\left\lvert\tilde{\psi}(t)\right\rangle = U_0^\dagger(t,t_0)\lvert\psi_S(t)\rangle$
$\rho_S(t) = U(t,t_0)\rho_S(t_0)U^\dagger(t,t_0)$	$\rho_H = \rho_S(t_0)$	$\tilde{\rho}(t) = U_0^\dagger(t,t_0)\rho_S(t)U_0(t,t_0)$
$A_S = A_H(t_0)$	$A_H(t) = U^\dagger(t,t_0)A(t_0)U(t,t_0)$	$\tilde{A}(t) = U_0^\dagger(t,t_0)A_S U_0(t,t_0)$
$\dot{\rho}_S(t) = -i\left[H,\rho_S(t)\right]$	$\dot{A}_H(t) = i\left[H,A_H(t)\right]$	$\dot{\tilde{\rho}}(t) = -i\left[\tilde{H}_I(t),\tilde{\rho}(t)\right]$

Table 2.1.: Relations between the different formulations of quantum mechanics

explicit than in Tab. 2.1. In appendix A.3 we derive the following relation:

$$\begin{aligned}\dot{\rho}_S(t) &= -\frac{i}{\hbar}\left[H_0,\rho_S(t)\right] + U_0(t,t_0)\dot{\tilde{\rho}}(t)U_0^\dagger(t,t_0)\\ &= -\frac{i}{\hbar}\left[H,\rho_S(t)\right] + U_0(t,t_0)\mathcal{D}\tilde{\rho}(t)U_0^\dagger(t,t_0),\end{aligned} \tag{2.11}$$

where $\mathcal{D}\tilde{\rho}(t)$ is the dissipative (i.e. non-Hamiltonian) part of the master equation (e.g. Lindblad operators).

2.3. Fermionic Creation and Annihilation Operators

In this thesis we deal with models consisting of discrete fermionic levels which we will describe using second quantization, i.e. fermionic creation and annihilation operators creating and destroying a particle in their respective level.

The operators corresponding to the ith system level will be denoted by d_i and $d_i^\dagger$, whereas we shall denote operators regarding the qth environmental mode belonging to the ith bath as $c_{i,q}$ $c_{i,q}^\dagger$.

The operators fulfill the following anticommutation relations:

$$\begin{array}{lcllcl}\{d_i,d_j\} &=& 0 & \{c_{i,q},c_{j,p}\} &=& 0\\ \{d_i,c_{j,q}^\dagger\} &=& 0 & \{d_i,c_{j,q}\} &=& 0\\ \{d_i,d_j^\dagger\} &=& \delta_{ij} & \{c_{i,q},c_{j,p}^\dagger\} &=& \delta_{ij}\delta_{qp}\end{array} \tag{2.12}$$

For general properties of commutators and anticommutators for fermionic operators refer to appendix A.1. For the interaction picture representation of these operators refer to appendix A.2.

3. Quantum Master Equations

In this chapter we discuss the time evolution of open quantum systems. To this end we first define what we mean by the term *open quantum system*. We will then introduce the concepts of dynamical maps and Markovian dynamics and concentrate on the class of universal dynamical maps (UDMs). Finally we will introduce quantum master equations (QME) and the Lindblad form which holds some remarkable properties.

As this is also standard textbook material we will only give a brief overview of the most important results and refer to the literature where appropriate. In our presentation we will closely follow [4, Chap. 3] for the general concepts and [5] for the more mathematical parts and also adopt their notation.

3.1. Open Quantum Systems

An open quantum system is a quantum system S (hereafter simply referred to as *system*) which is coupled to a second quantum system B called the *environment* [4]. We assume that both systems together form a closed system that can be described by unitary dynamics as presented in the last chapter. Their combined Hilbert space $\mathcal{H}$ is given by the tensor product of their respective Hilbert spaces $\mathcal{H} = \mathcal{H}_S \otimes \mathcal{H}_B$ and their state is characterized by the combined density matrix $\rho(t)$ (see figure 3.1). The Hamiltonian governing its time evolution is chosen to have to following form:

$$H(t) = H_S \otimes \mathbb{1}_B + \mathbb{1}_S \otimes H_B + H_I(t), \tag{3.1}$$

where $H_\alpha(\alpha = S, B)$ describes the internal dynamics of system and environment respectively and $H_I(t)$ describes the coupling between the two parts. The dynamics of the system S is therefore due to its internal dynamics and the interaction with the environment. The interaction will, in general, give rise to system-environment-correlations even though we might have started with a product-state. It is due to this fact that the time evolution of the system alone cannot be described in terms of Hamiltonian dynamics anymore.

The reduced state of the system (i.e. without accounting for the degrees of freedom of the environment) is obtained by taking the partial trace over the environment:

$$\rho_S(t) = \mathrm{tr}_B \rho(t) \tag{3.2}$$

Due to this operation the reduced density matrix $\rho_S(t)$ can (and in general will) be in a mixed state, even if the total system $\rho(t)$ is in a pure state.

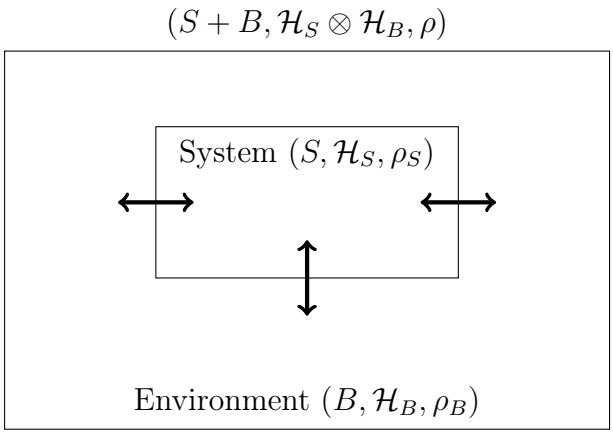

Figure 3.1.: Picture of an open quantum system. The arrows indicate different couplings of the bath to the environment.
After [4, Fig. 3.1]

3.2. Time Evolution and Dynamical Maps

As has been stated before, the time evolution of the reduced system can, in general, not be described by unitary time evolution. We can, however, determine its time evolution by considering the unitary evolution of the entire system and tracing over the degrees of freedom of the environment:

$$\rho_S(t_1) = \mathrm{tr}_B[U(t_1, t_0)\rho(t_0)U^\dagger(t_1, t_0)], \tag{3.3}$$

where $U(t_1, t_0)$ is the unitary evolution generated by the Hamiltonian $H(t)$ of the entire system.
This equation can be rewritten in terms of a dynamical map acting only on the Hilbert space of the reduced system:

$$\mathcal{E}_{t_1,t_0} : \rho_S(t_0) \to \rho_S(t_1) \tag{3.4}$$

$$\begin{array}{ccc} \rho(t_0) & \xrightarrow{U(t_1,t_0)} & \rho(t_1) \\ \mathrm{tr}_B \downarrow & & \downarrow \mathrm{tr}_B \\ \rho_S(t_0) & \xrightarrow[\mathcal{E}_{t_1,t_0}]{} & \rho_S(t_1) \end{array}$$

Figure 3.2.: Dynamical maps and their relation to unitary evolution of the entire system.
After [5, Chap. 4, Fig. 2]

This map will, in general, depend on the global unitary evolution, on the properties of the environment B and those of the reduced system S. It can, however, be shown, that there exist so-called *universal dynamical maps (UDMs)* which are defined to be

dynamical maps that are independent of the state they act upon [5]. We quote the following theorem whose proof can also be found in the stated reference.

Theorem 1 (cf. [5, Thm. 4.3])**.** *A dynamical map is a UDM iff it is induced from an extended system with the initial condition* $\rho(t_0) = \rho_S(t_0) \otimes \rho_B(t_0)$ *where* $\rho_B(t_0)$ *is fixed for any* $\rho_S(t_0)$

Therefore, if we are able to choose the state of the system and the environment to be uncorrelated for an initial time t_0, the dynamical map describing the evolution of the reduced system from that point in time to any later time t_1, will be independent of the initial state of the reduced system. This is, however, only exactly true for this specific t_0 as for times t with $t > t_0$ correlations arise such that the global state does not factorize anymore. It might, however, be possible that for weak system-environment interactions the global state still factorizes approximately for later times. This property is called *Markovianity* and can be defined as follows [5]:

Definition 1 (cf. [5, Def. 4.1])**.** *We will say that a quantum system undergoes a Markovian evolution if it is described by a contractive evolution family*[1] *on* $\mathfrak{B}$ *and satisfies the law of composition for the UDMs:*

$$\mathcal{E}_{t_2,t_0} = \mathcal{E}_{t_2,t_1}\mathcal{E}_{t_1,t_0} \tag{3.5}$$

The conditions under which this Markovian assumption holds will be discussed further when we discuss the microscopic derivations of quantum master equations.

With the Markovian property at hand we can now introduce the concept of a master-equation mathematically [5, Sect. 5.2]:

Definition 2. *A linear differential equation for* $\rho(t)$ *is called a master equation with generator* $\mathcal{L}_t$ *where*

$$\frac{d}{dt}\rho(t) = \lim_{\epsilon\to 0^+} \frac{\rho(t+\epsilon) - \rho(t)}{\epsilon} = \lim_{\epsilon\to 0^+} \frac{\mathcal{E}_{t+\epsilon,t} - \mathbb{1}}{\epsilon}\rho(t) \equiv \mathcal{L}_t\rho(t) \tag{3.6}$$

Note that if the UDMs only depend on time differences, $\mathcal{E}_{t_2,t_1} = \mathcal{E}_\tau$ with $\tau = t_2 - t_1$, they form a one-parameter semigroup. These semigroups can have an important property (from a physical point of view): the existence of a steady state.

Definition 3 (cf. [5, Def. 5.3])**.** *A semigroup* $\mathcal{E}_\tau$ *is relaxing if there exists a unique (steady) state* ρ_{SS} *such that* $\mathcal{E}_\tau(\rho_{SS}) = \rho_{SS}$ *for all* τ *and*

$$\lim_{\tau\to\infty}(\rho) = \rho_{SS} \tag{3.7}$$

for every initial state ρ

Having introduced these properties one may ask which semigroups are relaxing and

[1] i.e. $\|\mathcal{E}\|_1 \leq 1$, where $\|\cdot\|_1$ is the induced trace norm in $\mathfrak{B}^*$

what are their generators. The answer to both questions will concern us in the next section and will lead us to the introduction of the so-called *Lindblad* master equation.

3.3. The Lindblad Quantum Master Equation

In this section we introduce the Lindblad form of a master equation and quote two central theorems that underline the importance of the Lindblad form in describing dissipative dynamics.

The general ([4]) Lindblad form of a master equation is given by equation (3.8), where H is a (Hermitian) Hamiltonian and $\{V_k\}_k$ are so-called Lindblad operators such that for every operator its hermitian conjugate is also in the set labeled by k. The constants $\gamma_k \geq 0$ are called decay constants.

$$\frac{d}{dt}\rho(t) = -i\,[H, \rho(t)] + \sum_k \gamma_k \left[V_k \rho(t) V_k^\dagger - \frac{1}{2}\{V_k^\dagger V_k, \rho(t)\} \right] \tag{3.8}$$

Introducing superoperators as for the unitary evolution of closed quantum systems (cf. section 2.1) we can write the Lindblad QME in short as

$$\mathcal{L}\rho(t) \equiv -i\,[H, \rho(t)] + \mathcal{D}\rho(t), \tag{3.9}$$

where $\mathcal{L}$ is called Lindbladian and $\mathcal{D}$ is the dissipator of the QME.

We quote two theorems underlining the importance of the Lindblad form from [5]. A sketch of their proofs as well as further references can be found in the cited literature.

Theorem 2 (cf. [5, Thm. 5.1])**.** *A differential equation is a Markovian master equation iff it can be written in the form*

$$\frac{d}{dt}\rho(t) = -i\,[H(t), \rho(t)] + \sum_k \gamma_k(t) \left[V_k(t) \rho(t) V_k^\dagger(t) - \frac{1}{2}\{V_k^\dagger(t) V_k(t), \rho(t)\} \right] \tag{3.10}$$

where $H(t)$ and $V_k(t)$ are time-dependent operators, with $H(t)$ self-adjoint and $\gamma_k(t) \geq 0$ for every k and every t.

Theorem 3 (Spohn, cf. [5, Thm. 5.5])**.** *Consider a completely positive semigroup, $\mathcal{E}_\tau = e^{\mathcal{L}\tau}$, with generator*

$$\mathcal{L}[\cdot] = -i\,[H(t), \cdot] + \sum_{k \in I} \gamma_k \left[V_k [\cdot] V_k^\dagger - \frac{1}{2}\{V_k^\dagger V_k, \cdot\} \right] \tag{3.11}$$

for some set of indices I. Provided that the set $\{V_k, k \in I\}$ is self-adjoint (this is, the adjoint of every element of the set is inside of the set) and the only operators commuting with all of them are proportional to the identity, the semigroup $\mathcal{E}_\tau$ is relaxing.

To summarize, the Lindblad master equation has the following important properties:

- It is relaxing (see above)
- It preserves hermicity and positivity (see above)
- It preserves the trace of the density matrix

  Proof.

$$\begin{aligned}\mathrm{tr}\dot{\rho} &= \mathrm{tr}(\mathcal{L}\rho) \\ &= \mathrm{tr}\left(-i\left[H(t),\rho\right] + \sum_{k\in I}\gamma_k\left[V_k\rho V_k^\dagger - \frac{1}{2}\{V_k^\dagger V_k,\rho\}\right]\right) \\ &= 0\end{aligned}$$

  Where the last equality holds due to the cyclic property of the trace. □

- It is invariant under unitary transformations U [4, Eq. (3.72)]

$$\sqrt{\gamma_k}V_k \to \sqrt{\gamma_k'}V_k' = \sum_{j=1}^{N^2-1} U_{kj}\sqrt{\gamma_j}V_j,$$

  where U_{ij} is a unitary matrix

- It is invariant under the following inhomogeneous transformation [4, Eq. (3.73)]

$$\begin{aligned}V_k &\to V_k' = V_k + a_k \\ H &\to H' = H + \frac{1}{2i}\sum_k \gamma_k(a_k^* V_k - a_k V_k^\dagger) + b,\end{aligned}$$

  where $a_k \in \mathbb{C}, b \in \mathbb{R}$.

  Due to this property we can always choose the Lindblad operators to be traceless.

4. General Derivation from Microsopic Models

In this chapter we outline the general procedure to derive a Lindblad master equation from a microscopic model. Again we closely follow [4, Chap. 3] and [5] and part of the notation as well as of the calculations has been taken from [6, Sec 7.2 and 7.3].

As has been stated before, the Hilbert space of the entire system we consider is given by

$$\mathcal{H} = \mathcal{H}_S \otimes \mathcal{H}_B, \tag{4.1}$$

and its dynamics is described by a Hamiltonian of the form (3.1)

$$H_{\text{total}} = H_0 + \alpha H_I = H_S + H_B + \alpha H_I, \tag{4.2}$$

where H_0 denotes the free evolution of the system and the environment. α is a parameter determining the strength of the interaction which will later on be used as an expansion parameter. In the models we consider α will be the coupling strength of the levels to the Lindblad drive.

4.1. Properties of the Baths

In our models we will assume the environment to consist of different baths each coupled to, in general, various system levels. Each bath i consists of infinitely many modes q and we assume it to be in the stationary thermal state with respect to its temperature T_i:

$$\tilde{\rho}_{B,i}(t) = \rho_{B,i}(0) \equiv \rho_{0,i} = \frac{\exp(-H_{B,i}/kT)}{\text{tr}_{B_i} \exp(-H_{B,i}/kT_i)}, \tag{4.3}$$

where the Hamiltonian of the bath will in general be given by:

$$H_B = \sum_q \omega_q c_q^\dagger c_q \tag{4.4}$$

In order to characterize the bath we introduce the spectral density $J(\omega)$ such that the sum over all modes q can be replaced by an integral over the entire frequency space:

$$H_B = \int_{-\infty}^{\infty} d\omega \rho(\omega) c_\omega^\dagger c_\omega \omega \tag{4.5}$$

with density of states

$$\rho(\omega) = \sum_q \delta(\omega - \omega_q). \tag{4.6}$$

As it will become useful later on, we introduce the spectral density $J(\omega)$ as follows:

$$J(\omega) = V^2 \sum_q \delta(\omega - \omega_q) \tag{4.7}$$

In our models we assume that the bath modes are equally spaced and consider the wide-band limit such that we can assume a constant spectral density

$$J(\omega) = V^2 \rho(\omega) \equiv V^2 \rho. \tag{4.8}$$

In Chap. 7 we will introduce the level width function Γ which, under our assumptions, is also constant and given by:

$$\frac{\Gamma(\omega)}{2} = \pi J(\omega) \equiv \pi J \tag{4.9}$$

Moreover, as the bath is in the stationary thermal state, the following two properties will – at least for the models we consider – be true, for the interaction Hamiltonian contains only one bath creation or annihilation operator (Eq. 4.10) and the thermal state is diagonal in the basis of H_B (Eq. 4.11).

$$\mathrm{tr}_B \left(\tilde{H}_I(t) \rho_0 \right) = 0 \tag{4.10}$$

$$[H_B, \rho_0] = 0 \tag{4.11}$$

4.2. Projection Operator Method

We shall now derive a master equation in what is referred to in the literature as Born approximation [4, Chap. 3.3], using projection operator methods. This method is named after Nakajima and Zwanzig and outlined in [5] and [7] whose derivation we shall follow closely. For further details and references refer to them. Note, that there is another possibility to derive this equation without making use of projection operators. We shall present this derivation in appendix A.4.

Let as start by defining two orthogonal projection operators on $\mathcal{H}$:

$$\mathcal{P}\rho = \mathrm{tr}_B(\rho) \otimes \rho_0 \tag{4.12}$$

$$\mathcal{Q}\rho = (\mathbb{1} - \mathcal{P})\rho \tag{4.13}$$

For the Liouville-von Neumann equation in the interaction picture (see Tab. 2.1) we introduce the following notation:

$$\frac{d}{dt}\tilde{\rho} = -i\alpha \left[\tilde{H}_I(t), \tilde{\rho}(t) \right] \equiv \alpha \mathcal{V}(t) \tilde{\rho}(t) \tag{4.14}$$

The equilibrium property (4.10) of the bath thus reads

$$\mathcal{P}\mathcal{V}(t)\mathcal{P} = 0 \tag{4.15}$$

Introducing the identity $\mathbb{1} = \mathcal{P} + \mathcal{Q}$ into the Liouville-von Neumann equation leads to

$$\frac{d}{dt}\mathcal{P}\tilde{\rho}(t) = \alpha\mathcal{P}\mathcal{V}(t)\mathcal{P}\tilde{\rho}(t) + \alpha\mathcal{P}\mathcal{V}(t)\mathcal{Q}\tilde{\rho}(t) \tag{4.16}$$

$$\frac{d}{dt}\mathcal{Q}\tilde{\rho}(t) = \alpha\mathcal{Q}\mathcal{V}(t)\mathcal{P}\tilde{\rho}(t) + \alpha\mathcal{Q}\mathcal{V}(t)\mathcal{Q}\tilde{\rho}(t) \tag{4.17}$$

The formal solution of (4.17) is given by:

$$\mathcal{Q}\tilde{\rho}(t) = \mathcal{G}(t,t_0)\mathcal{Q}\tilde{\rho}(t_0) + \alpha\int_{t_0}^{t} ds\mathcal{G}(t,s)\mathcal{Q}\mathcal{V}(s)\mathcal{P}\tilde{\rho}(s) \tag{4.18}$$

Where the propagator of the homogeneous equation is given by:

$$\mathcal{G}(t,s) = \mathcal{T}\exp\left(\alpha\int_{s}^{t} d\tau\mathcal{Q}\mathcal{V}(\tau)\right) \tag{4.19}$$

Inserting this into equation (4.16) yields:

$$\frac{d}{dt}\mathcal{P}\tilde{\rho}(t) = \alpha\mathcal{P}\mathcal{V}(t)\mathcal{P}\tilde{\rho}(t) + \alpha\mathcal{P}\mathcal{V}(t)\mathcal{G}(t,t_0)\mathcal{Q}\tilde{\rho}(t_0) + \alpha^2\int_{t_0}^{t} ds\mathcal{P}\mathcal{V}(t)\mathcal{G}(t,s)\mathcal{Q}\mathcal{V}(s)\mathcal{P}\tilde{\rho}(s) \tag{4.20}$$

We now make the assumption (see Thm. 1) that the state factorizes at time t_0, an assumption that is necessary for the evolution to be a universal dynamical map: $\rho(t_0) = \rho_S(t_0)\otimes\rho_0(t_0)$. This gives by definition $\mathcal{Q}\rho(t_0) = 0$ and by using the equilibrium property of the bath (4.15) we arrive at:

$$\frac{d}{dt}\mathcal{P}\tilde{\rho}(t) = \int_{t_0}^{t} ds\mathcal{K}(t,s)\mathcal{P}\tilde{\rho}(s) \tag{4.21}$$

with kernel

$$\mathcal{K}(t,s) = \alpha^2\mathcal{P}\mathcal{V}(t)\mathcal{G}(t,s)\mathcal{Q}\mathcal{V}(s)\mathcal{P}. \tag{4.22}$$

In the weak coupling limit we expand the kernel to lowest order in α which finally leads to:

$$\frac{d}{dt}\mathcal{P}\tilde{\rho}(t) = \alpha^2\int_{t_0}^{t} ds\mathcal{P}\mathcal{V}(t)\mathcal{V}(s)\mathcal{P}\tilde{\rho}(s) \tag{4.23}$$

$$= -\alpha^2\int_{t_0}^{t} ds\mathrm{tr}_B\left[\tilde{H}_I(t),\left[\tilde{H}_I(s),\tilde{\rho}_S(s)\otimes\rho_0\right]\right]\otimes\rho_0 \tag{4.24}$$

Replacing s by $t-s$ and setting $t_0 = 0$ we finally arrive at:

$$\frac{d}{dt}\tilde{\rho}_S(t) = -\alpha^2\int_{0}^{t} ds\mathrm{tr}_B\left[\tilde{H}_I(t),\left[\tilde{H}_I(t-s),\tilde{\rho}_S(t-s)\otimes\rho_0\right]\right] \tag{4.25}$$

Note that a similar derivation can be done for the case of several baths. We shall comment on this later on. Note further, that we only made the factoring assumption for the initial time t_0 and its prevalence for later times $t > t_0$ arises merely due to our expansion to lowest order in the interaction. For the alternative derivation (cf. appendix A.4) the factoring assumption has to be extended for later times by argument and it is for this reason that we stated the projection operator method.

4.3. Bath Correlation Functions

In order to evaluate the above integral we have to invoke a final approximation, the so-called Markov approximation, which will be introduced in the next section. In order to justify this approximation we now consider the bath correlation function and calculate its decay over time using the residue theorem.

The bath correlation function will be denoted by $C(t,t')$ and is defined as:

$$C(t,t') = \mathrm{tr}_B \left\{ \sum_{q,q'} \tilde{c}_q^\dagger(t) \tilde{c}_{q'}(t') \rho_0 \right\} \tag{4.26}$$

Due to properties (4.10) and (4.11) of the bath the correlation function only depends on the difference $\tau = t - t'$ and only terms with $q = q'$ contribute:

$$\begin{aligned} C(t,t') = \mathrm{tr}_B \left\{ \sum_{q,q'} \tilde{c}_q^\dagger(t) \tilde{c}_{q'}(t') \rho_0 \delta_{qq'} \right\} &\overset{(4.11)}{=} \mathrm{tr}_B \left\{ \sum_{q} \tilde{c}_q^\dagger(t-t') c_{q'} \rho_0 \right\} \\ &\equiv C(t-t') \\ &\equiv C(\tau) \end{aligned} \tag{4.27}$$

Using the residue theorem and the interaction picture representation of the operators we obtain[1]:

$$C(\tau) = \mathrm{tr}_B \left\{ \sum_q \tilde{c}_q^\dagger(\tau) c_q \rho_0 \right\} = \int_{-\infty}^{\infty} d\omega e^{i\omega\tau} f(\omega) \rho(\omega) \tag{4.28}$$

$$= \rho \int_{-\infty}^{\infty} d\omega \frac{e^{i\omega\tau}}{e^{\omega/T} + 1} \tag{4.29}$$

$$= -\rho i T \frac{1}{\sinh(\pi T \tau)}, \tag{4.30}$$

where $f(\omega)$ denotes the Fermi-Dirac-distribution with respect to the temperature T of the bath.

The bath correlation function is therefore peaked around $\tau = t - t' = 0$ and decays on a timescale proportional to the inverse temperature. It is this property that will allow us to invoke the Markov assumption to our problems so that the evolution of the

[1] For a detailed derivation refer to appendix A.5

system does no longer depend on its past but only on its current state. If the density matrix evolves on a timescale Γ^{-1} this Markov approximation is valid for the regime $\Gamma/T \ll 1$ as for these timescales there will not be any memory effects.

4.4. The Markov Approximation

The master equation in Born approximation (4.25) cannot be solved easily due to two reasons: First, it is not local in time as the reduced density matrix still depends on the entire history of the problem (as its time-argument on the right hand side still depends on s). Second, the integration runs to time t.

Both these problems can be resolved by imposing the Markov assumption onto our system. This, as has been quoted in Thm. 2, is a necessary condition to arrive at a QME in Lindblad form. In physical terms the Markov approximation is the assumption that memory effects do not play an important role and that therefore the evolution of the reduced density matrix only depends on its current state and not on its past [4, Sec. 3.2].

We will see (cf. for example Eq. 5.3) that the interaction Hamiltonian appearing in Eq. (4.25) separates in two parts: a bath correlation function and a part containing system operators and the reduced density matrix. As has been shown above the bath correlation function $C(\tau)$ is sharply peaked around the value $\tau = t - t' = 0$ where the width of the peak $\delta\tau$ is much smaller than the timescale τ_R on which the reduced density matrix changes substantially ($\delta\tau \ll \tau_R$). Following [4, 8] we therefore invoke the following approximations to equation (4.25): First, the reduced density matrix on the right can be made local in time by replacing $(t - s)$ by t due to its slow evolution compared to the bath correlation functions. Only small times (of order $\delta\tau$) will contribute to the integral and on this timescale the reduced density matrix can be viewed as a constant. Note, that this assumption has to be checked for the different models at hand and that the argument given here is only strictly valid for the resonant level model discussed in the next section. Second, the integration can be extended to infinity as times larger than the bath-correlation time will not contribute to the integral. We finally obtain the quantum master equation in Born-Markov approximation which will be the starting point for our later derivations:

$$\frac{d}{dt}\tilde{\rho}_S(t) = -\int_0^\infty ds \mathrm{tr}_B \left[\tilde{H}_I(t), \left[\tilde{H}_I(t-s), \rho_S(t) \otimes \rho_0\right]\right] \tag{4.31}$$

Expanding the double commutator and regrouping the terms we arrive at a form which will become useful in the following[2]:

$$\frac{d}{dt}\tilde{\rho}_S(t) = -\int_0^\infty ds \mathrm{tr}_B \left\{\tilde{H}_I(t)\tilde{H}_I(t-s)\tilde{\rho}_S(t)\rho_0 - \tilde{H}_I(t-s)\tilde{\rho}_S(t)\rho_0\tilde{H}_I(t) + \mathrm{h.c.}\right\} \tag{4.32}$$

Note, that from this point on we drop the tensor product symbol in order to simplify

[2]For a short derivation see appendix A.6

notation. So far we still deal with interaction picture operators. After plugging in concrete examples for the interaction we will eventually go back to the Schrödinger picture.

5. The Resonant Level Model

In this and the following chapters we will use the general procedure outlined before in order to derive quantum master equations in Lindblad form for different fermionic open quantum systems. The general approach and part of the notation have been inspired by [4, Sec. 3.3], [5], [6, Sec. 7.1 ff.] and [7], where the authors consider bosonic systems that are similar to ours.

5.1. Description of the Model

As a first example we will consider an easy model consisting of one level of energy Ω coupled to an environment consisting of an infinite number of levels q with energy ω_q. In the following we shall assume the coupling to the bath-modes to be homogeneous and will choose the coupling-constant V to be real. The Hamiltonian for this so-called resonant level model is given by equation (5.1) and a graphical illustration of the model is shown in Fig. 5.1.

$$\begin{aligned} H = H_S + H_B + H_I &= \Omega d^\dagger d + \sum_q \omega_q c^\dagger c + \sum_q \left(V_q c_q^\dagger d + V_q^* d^\dagger c_q \right) \\ &\equiv \Omega d^\dagger d + \sum_q \omega_q c^\dagger c + V \sum_q \left(c_q^\dagger d + d^\dagger c_q \right) \end{aligned} \tag{5.1}$$

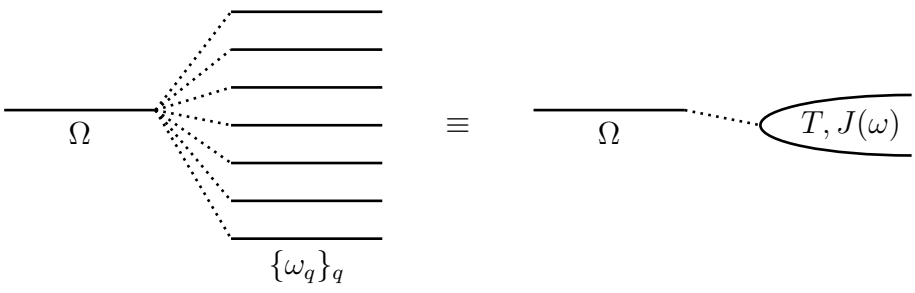

Figure 5.1.: Two schematic pictures of the resonant level model. All the bath modes are combined to a bath with temperature T and spectral density $J(\omega)$

5.2. Quantum Master Equation

On deriving the Lindblad master equation for the resonant level model we shall start from the QME in the Born-Markov approximation. This approximation has already

been discussed for this simple model in the previous chapters.

The interaction-picture representation[1] of the above operators is given by[2]

$$\begin{aligned} \tilde{d}^\dagger(t) &= e^{i\Omega t}d^\dagger & \tilde{d}(t) &= e^{-i\Omega t}d \\ \tilde{c}_q(t) &= e^{-i\omega_q t}c_q & \tilde{c}_q^\dagger(t) &= e^{i\omega_q t}c_q^\dagger \end{aligned} \tag{5.2}$$

Upon substituting these operators into QME (4.32) we arrive at:

$$\begin{aligned} \frac{d}{dt}\tilde{\rho}_S(t) &= -\int_0^\infty ds \mathrm{tr}_B \left\{ \tilde{H}_I(t)\tilde{H}_I(t-s)\tilde{\rho}_S(t)\rho_0 - \tilde{H}_I(t-s)\tilde{\rho}_S(t)\rho_0\tilde{H}_I(t) + \mathrm{h.c.} \right\} \\ &= -V^2 \sum_{q,q'} \int_0^\infty ds \mathrm{tr}_B \Big\{ \tilde{c}_q^\dagger(t)\tilde{c}_{q'}(t-s)\tilde{d}(t)\tilde{d}^\dagger(t-s)\tilde{\rho}_S(t)\rho_0 \\ &\qquad + \tilde{c}_q(t)\tilde{c}_{q'}^\dagger(t-s)\tilde{d}^\dagger(t)\tilde{d}(t-s)\tilde{\rho}_S(t)\rho_0 \\ &\qquad - \tilde{c}_{q'}^\dagger(t-s)\rho_0\tilde{c}_q(t)\tilde{d}(t-s)\tilde{\rho}_S(t)\tilde{d}^\dagger(t) \\ &\qquad - \tilde{c}_{q'}(t-s)\rho_0\tilde{c}_q^\dagger(t)\tilde{d}^\dagger(t-s)\tilde{\rho}_S(t)\tilde{d}(t) + \mathrm{h.c.} \Big\} \\ &= -V^2 \sum_{q,q'} \int_0^\infty ds \Big\{ \mathrm{tr}_B \left(\tilde{c}_q^\dagger(s)\tilde{c}_{q'}\rho_0 \right) \left(\tilde{d}(t)\tilde{d}^\dagger(t-s)\tilde{\rho}_S(t) - \tilde{d}^\dagger(t-s)\tilde{\rho}_S(t)\tilde{d}(t) \right) \\ &\qquad + \mathrm{tr}_B \left(\tilde{c}_q(s)\tilde{c}_{q'}^\dagger\rho_0 \right) \left(\tilde{d}^\dagger(t)\tilde{d}(t-s)\tilde{\rho}_S(t) - \tilde{d}^\dagger(t)\tilde{\rho}_S(t)\tilde{d}(t-s) \right) \\ &\qquad + \mathrm{h.c.} \} \end{aligned} \tag{5.3}$$

At this point we introduce the spectral density defined above (4.7) and use the explicit form of the operators in the interaction picture and the bath correlation functions to finally obtain:

$$\begin{aligned} \frac{d}{dt}\tilde{\rho}_S(t) = -\int_{-\infty}^\infty J(\omega)d\omega \Big\{ & f(\omega) \int_0^\infty ds e^{-i(\Omega-\omega)s} \left(\tilde{d}(t)\tilde{d}^\dagger(t)\tilde{\rho}_S(t) - \tilde{d}^\dagger(t)\tilde{\rho}_S(t)\tilde{d}(t) \right) \\ & + (1-f(\omega)) \int_0^\infty ds e^{i(\Omega-\omega)s} \left(\tilde{d}^\dagger(t)\tilde{d}(t)\tilde{\rho}_S(t) - \tilde{d}^\dagger(t)\tilde{\rho}_S(t)\tilde{d}(t) \right) + \mathrm{h.c.} \Big\} \end{aligned} \tag{5.4}$$

We now make use of the following formula (see for example [9, Note 1.2]) in order to evaluate the integration with respect to s

$$\int_0^\infty dk e^{\pm ikx} = \pi\delta(x) \pm i\mathcal{P}\left(\frac{1}{x}\right), \tag{5.5}$$

where $\mathcal{P}$ denotes the principal value.

[1] By interaction picture we mean the interaction picture with respect to the free evolution of the system- and bath-modes

[2] For a derivation cf. appendix (A.2)

After some algebra and having gone back to the Schrödinger picture (cf. 2.11) we obtain the following master equation which is in Lindblad form.

$$\frac{d}{dt}\rho_S(t) = -i(\Omega + \overbrace{\Delta_- - \Delta_+}^{\mathcal{P}\int_{-\infty}^{\infty} d\omega \frac{J(\omega)}{\Omega-\omega}}) \left[d^\dagger d, \rho_S(t)\right] + \gamma_- \left(2d\rho_S(t)d^\dagger - d^\dagger d\rho_S(t) - \rho_S(t)d^\dagger d\right) + \gamma_+ \left(2d^\dagger\rho_S(t)d - dd^\dagger\rho_S(t) - \rho_S(t)dd^\dagger\right), \tag{5.6}$$

where

$$\begin{aligned} \gamma_- &= \pi J(\Omega)(1-f(\Omega)) & \Delta_- &= \mathcal{P}\int_{-\infty}^{\infty} d\omega \frac{J(\omega)(1-f(\omega))}{\Omega-\omega} \\ \gamma_+ &= \pi J(\Omega) f(\Omega) & \Delta_+ &= -\mathcal{P}\int_{-\infty}^{\infty} d\omega \frac{J(\omega)f(\omega)}{\Omega-\omega} \end{aligned} \tag{5.7}$$

The principal value integral in the Hamiltonian part of the QME is usually referred to as Lamb-Shift [8] and can be shown to vanish in our model:

$$\lim_{D\to\infty} \mathcal{P}\int_{-D}^{D} d\omega \frac{J(\omega)}{\Omega-\omega} = J \lim_{D\to\infty} \ln\left(\frac{|\Omega - D|}{|\Omega + D|}\right) = 0, \tag{5.8}$$

where we have assumed that J is constant.

5.3. Equilibrium Properties: Thermalization Behavior

In the following we shall discuss the equilibrium dynamics of the derived QME. Let us calculate the evolution of the expectation value of the occupation number:

$$\begin{aligned} \frac{d}{dt}\left\langle d^\dagger d\right\rangle &= \mathrm{tr}_S(d^\dagger d\mathcal{L}\rho_S(t)) \\ &= -2(\gamma_- + \gamma_+)\left\langle d^\dagger d\right\rangle + 2\gamma_+ \end{aligned} \tag{5.9}$$

In the steady state, this time derivative has to vanish. This gives rise to the mean occupation number in the steady state:

$$\left\langle d^\dagger d\right\rangle_{\mathrm{SS}} = \frac{\gamma_+}{\gamma_- + \gamma_+} = f(\Omega) \tag{5.10}$$

where all the prefactors cancel and we are left with the Fermi distribution function evaluated at the energy Ω of the level. The single level coupled to an infinite number of bath modes therefore correctly thermalizes to its thermal occupation according to the temperature of the bath:

$$\rho_{SS} = \begin{pmatrix} f(\Omega,T) & 0 \\ 0 & 1-f(\Omega,T) \end{pmatrix} \tag{5.11}$$

We note that this steady state is a mixed state that shows no coherence, i.e. the off-diagonal terms in (5.11) are zero. Even if the system was initially in a pure state

$\rho_S(t=0) = |\psi\rangle\langle\psi|$ with, for example, $|\psi\rangle = \frac{1}{\sqrt{2}}|0\rangle + \frac{i}{\sqrt{2}}|1\rangle$ the correlations would die out and the system would reach the mixed steady state.

The time evolution for the coherences can be derived similarly to the occupation:

$$\begin{aligned}\frac{d}{dt}\langle d\rangle &= \mathrm{tr}_S(d\mathcal{L}\rho_S(t)) \\ &= -(\gamma_- + \gamma_+)\langle d\rangle - i\Omega\langle d\rangle\end{aligned} \tag{5.12}$$

From the two differential equations (5.9) and (5.12) we arrive at the following equations of motion:

$$\langle d\rangle(t) = \langle d\rangle(0)e^{-i\Omega t-\gamma t} \tag{5.13}$$

$$\langle N\rangle(t) = (\langle N\rangle(0) - f(\Omega,T))\,e^{-2\gamma t} + f(\Omega,T), \tag{5.14}$$

where we introduce $\gamma = \gamma_+ + \gamma_- = \pi J$.

A numerical simulation for the dynamics of the initial state mentioned above under the influence of the Lindblad bath is shown in Fig. 5.2. We can clearly see the exponential decay towards the steady state. The occupation decays with rate $2\gamma^{-1}$ (where $2\gamma = 2\pi V^2\rho$) and the coherences with half this rate. For unitary evolution, i.e. without the presence of the bath, the radius of the circle in Fig. 5.2 would stay constant.

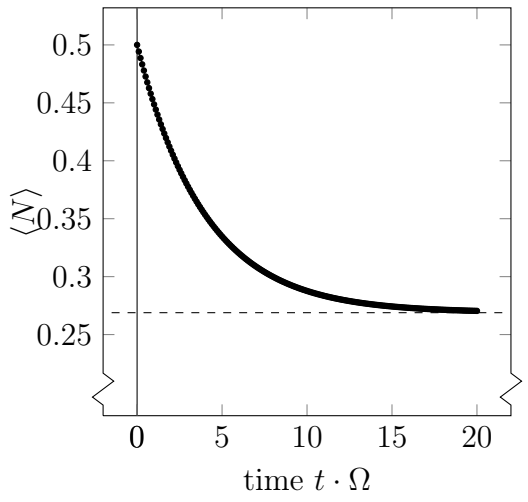

(a) Expectation value of the occupation $N = d^\dagger d$. It decays exponentially from its initial value 0.5 towards $f(\Omega,T)$ (dotted line) with inverse decay constant $2\gamma = 2\pi V^2\rho$

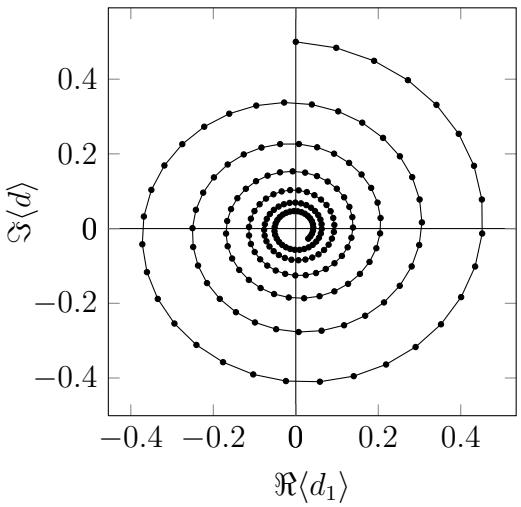

(b) Expectation value of the coherence d. It decays to 0 with decay constant $\gamma = \pi V^2\rho$. The separation between two adjacent dots is 0.1 time units.

Figure 5.2.: Dynamics of the state $\rho_S(t=0) = |\psi\rangle\langle\psi|$ with $|\psi\rangle = \frac{1}{\sqrt{2}}|0\rangle + \frac{i}{\sqrt{2}}|1\rangle$ under Lindblad drive. The parameters used are $\Omega = 1, T = 1\Omega, V = 0.2\Omega$.

6. Two Coupled Levels, one Bath

In this chapter an extension of the Resonant Level Model (cf. 5) will be considered. Two hybridized levels with energies Ω_1 and Ω_2 are coupled to a thermal bath via the second level. The system is depicted in Fig. 6.1 and the Hamiltonian is given by Eq. (6.1).

$$H = H_S + H_B + H_I \tag{6.1}$$

where

$$\begin{aligned} H_S &= H_1 + H_2 + H_{12} = \Omega_1 d_1^\dagger d_1 + \Omega_2 d_2^\dagger d_2 + g\left(d_1^\dagger d_2 + d_2^\dagger d_1\right) \\ H_B &= \sum_q \omega_q c_q^\dagger c_q \\ H_I &= V \sum_q \left(d_2^\dagger c_q + c_q^\dagger d_2\right) \end{aligned} \tag{6.2}$$

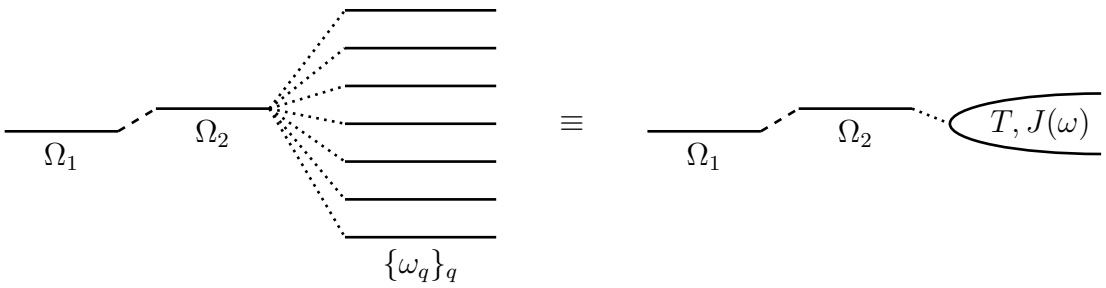

Figure 6.1.: Two schematic pictures of the considered model. All the bath modes are combined to a bath with temperature T and spectral density $J(\omega)$

Due to the coupling between the two system levels new dynamics arises and for a correct description we have to include Lindblad terms for the first level as well, as it is coupled to and thermalizes through the second system level. Similar bosonic systems are discussed for example by [8, 7]. As there, we have to decide how to deal with the coupling of the two levels as the Hamiltonian of the system is no longer diagonal in the basis chosen above[1]. In this chapter we therefore consider two different approaches to derive QMEs in Lindblad form and study their behavior. To this end we assume the Born-Markov approximation to hold also for our composite model and discuss this assumption at the end of the chapter.

[1] We will refer to this basis in the following as "local basis"

6.1. Quantum Master Equation in the Eigenbasis

In the following we derive a QME for the dynamics of the coupled subsystems described by H_S. As suggested in [5, Sect. 6.4] we include the coupling into the generating Hamiltonian of the interaction picture and derive the QME in the eigenbasis of the system Hamiltonian including this coupling. To this end we first diagonalize the Hamiltonian and derive creation and annihilation operators for the new eigenstates. The coupling of the second level to the bath via H_I is then expressed in terms of these new creation and annihilation operators (and those of the bath). In the new basis the interaction picture creation and annihilation operators will take a particularly simple form whereas the interaction picture operators corresponding to the original single level operators are very hard to calculate except for special cases (i.e. when the levels are degenerate in energy). Using similar techniques as before the QME is then calculated in the Born-Markov-approximation. In the end the coupled creation and annihilation operators are re-expressed by those of the individual subsystems.

The straightforward diagonalization of the problem is performed in appendix A.7. There we obtain the relation between the creation and annihilation operators in the eigenbasis and those of the local basis to be[2]:

$$\begin{pmatrix} D_+^\dagger \\ D_-^\dagger \end{pmatrix} = \underbrace{\begin{pmatrix} \frac{1}{\sqrt{1+\eta_+^2}} & \frac{\eta_+}{\sqrt{1+\eta_+^2}} \\ \frac{1}{\sqrt{1+\eta_-^2}} & \frac{\eta_-}{\sqrt{1+\eta_-^2}} \end{pmatrix}}_{=:A} \begin{pmatrix} d_1^\dagger \\ d_2^\dagger \end{pmatrix} \tag{6.3}$$

where

$$\eta_\pm = \frac{\Omega_2 - \Omega_1}{2g} \pm \sqrt{1 + \left(\frac{\Omega_2 - \Omega_1}{2g}\right)^2} \tag{6.4}$$

The interaction with the bath (6.2) can be rewritten so that it takes the same form as for the resonant model discussed before with an additional sum over n.

$$\begin{aligned} H_I &= V \sum_q \left(c_q^\dagger d_2 + d_2^\dagger c_q \right) \\ &= V \sum_q \sum_{n=\pm} \left(c_q^\dagger \left(A_{n2} D_n \right) + \left(A_{n2} D_n^\dagger \right) c_q \right) \\ &= \underbrace{\sum_{n=\pm} \left(A_{n2} D_n^\dagger \right)}_{\mathrm{S}_1} \otimes \underbrace{V \sum_q c_q}_{\mathrm{B}_1} + \underbrace{V \sum_q c_q^\dagger}_{\mathrm{B}_2} \otimes \underbrace{\sum_{n=\pm} \left(A_{n2} D_n \right)}_{\mathrm{S}_2} \end{aligned} \tag{6.5}$$

[2]For the components of the matrix A we from now on adapt the following notation:

$$A = \begin{pmatrix} A_{+1} & A_{+2} \\ A_{-1} & A_{-2} \end{pmatrix}$$

Starting from equation (4.32) and using exactly the same steps as before[3] we finally arrive at an equation that looks similar to the QME of the resonant level model.

$$\begin{aligned}\frac{d}{dt}\tilde{\rho}_S(t) = -\sum_{n,n'=\pm}\Big\{&A_{n2}A_{n'2}\left(\gamma_-(\Omega_{n'})+i\Delta_-(\Omega_{n'})\right)e^{i(\Omega_n-\Omega_{n'})t}\left(D_n^\dagger D_{n'}\tilde{\rho}_s(t)-D_{n'}\tilde{\rho}_s(t)D_n^\dagger\right)\\&+A_{n2}A_{n'2}\left(\gamma_+(\Omega_{n'})+i\Delta_+(\Omega_{n'})\right)e^{i(\Omega_{n'}-\Omega_n)t}\left(D_nD_{n'}^\dagger\tilde{\rho}_s(t)-D_{n'}^\dagger\tilde{\rho}_s(t)D_n\right)\\&+\text{h.c.}\Big\},\end{aligned} \tag{6.6}$$

where

$$\begin{array}{lcllcl}\gamma_-(\Omega_n) &=& \pi\left(1-f(\Omega_n)\right)J(\Omega_n) & \Delta_-(\Omega_n) &=& \mathcal{P}\int d\omega\frac{(1-f(\omega))J(\omega)}{\Omega_n-\omega}\\ \gamma_+(\Omega_n) &=& \pi f(\Omega_n)J(\Omega_n) & \Delta_+(\Omega_n) &=& -\mathcal{P}\int d\omega\frac{f(\omega)J(\omega)}{\Omega_n-\omega}\end{array} \tag{6.7}$$

However, due to the sum over n and n' it cannot be written in Lindblad form as the operator premultiplying the density matrix in the Lindblad term has to be the hermitian conjugate of the operator postmultiplying it. Note that the exponential terms would vanish when going back to the Schrödinger picture whereas the sums over n and n' remain.

In order to obtain a Lindblad form a further approximation has to be introduced which is referred to as secular approximation in the literature (cf. [8, Appendix], [7, chap. 3.2.2]). The exponentials with non-vanishing exponent in (6.6) evolve with frequencies $\pm(\Omega_+ - \Omega_-) = \pm 2\sqrt{g^2 + (\Omega_1 - \Omega_2)^2/4} \geq 2g$. If this oscillation occurs on timescales much shorter than those induced by the coupling of the second subsystem to the bath ($g \gg V$) these fast-oscillating terms can be neglected and only terms with $n = n'$ remain. This approximation is therefore only valid in the strong-coupling regime where the intersubsystem-coupling is (much) stronger than the coupling to the bath. Note that due to this averaging process the master equation obtained will no longer be able to describe the dynamics on timescales of the intersubsystem coupling [8].

The QME in the interaction picture in the coupled basis is hence given by:

$$\begin{aligned}\frac{d}{dt}\tilde{\rho}_S(t) = -\sum_{n=\pm}\Big\{&A_{n2}^2\left(\gamma_-(\Omega_n)+i\Delta_-(\Omega_n)\right)\left(D_n^\dagger D_n\tilde{\rho}_s(t)-D_n\tilde{\rho}_s(t)D_n^\dagger\right)\\&+A_{n2}^2\left(\gamma_+(\Omega_n)+i\Delta_+(\Omega_n)\right)\left(D_nD_n^\dagger\tilde{\rho}_s(t)-D_n^\dagger\tilde{\rho}_s(t)D_n\right)\\&+\text{h.c.}\Big\}\end{aligned} \tag{6.8}$$

As has been the case for the resonant level model, the complex terms (containing the expressions $\Delta_\pm$) will contribute to the unitary evolution of the state whereas the real terms (containing the expressions $\gamma_\pm$) will contribute to the dissipative dynamics.

[3] Plug in the interaction Hamiltonian in the interaction picture and collect all the terms for the bath-modes that will finally give rise to the bath correlation functions. Invoke the result (5.5) from distribution theory

Equation (6.8) can be written in Lindblad-form due to the secular approximation. Going back to the Schrödinger picture we obtain the Lindblad QME in the coupled basis:

$$\begin{aligned}\frac{d}{dt}\rho_S(t) = &-i\left[\Omega_+ D_+^\dagger D_+ + \Omega_- D_-^\dagger D_-, \rho_S(t)\right] \\ &+ \sum_{n=\pm} A_{n2}^2 \gamma_-(\Omega_n)\left(2D_n\rho_S(t)D_n^\dagger - \rho_S(t)D_n^\dagger D_n - D_n^\dagger D_n\rho_S(t)\right) \\ &+ \sum_{n=\pm} A_{n2}^2 \gamma_+(\Omega_n)\left(2D_n^\dagger\rho_S(t)D_n - \rho_S(t)D_nD_n^\dagger - D_nD_n^\dagger\rho_S(t)\right),\end{aligned} \tag{6.9}$$

where the decay rates $\gamma_\pm$ are defined as above and we have used the fact that the Lamb-Shift is zero for our model.

Before we discuss the properties of this master equation further, we express it in terms of single-level creation and annihilation operators. The resulting equation will still be in Lindblad form as the two bases are connected by a unitary transformation and, as has been stated in section 3.3, the Lindblad form is invariant under unitary transformations. Replacing the coupled creation and annihilation operators by those of the subsystems we arrive after some algebra at the following master equation for the single-level operators. It contains the Lindblad-terms containing only operators for one subsystem (given by K_{nn}^i) and those containing cross-terms:

$$\begin{aligned}\frac{d}{dt}\rho_S(t) = &-i\left[\overline{\Omega}_1 d_1^\dagger d_1 + \overline{\Omega}_2 d_2^\dagger d_2 + \overline{g}\left(d_1^\dagger d_2 + d_2^\dagger d_1\right), \rho_S(t)\right] \\ &- \sum_{m,m'=1}^{2} K_{mm'}^1\left(d_m^\dagger d_{m'}\rho_S(t) + \rho_S(t)d_m^\dagger d_{m'} - 2d_{m'}\rho_S(t)d_m^\dagger\right) \\ &- \sum_{m,m'=1}^{2} K_{mm'}^2\left(d_{m'}d_m^\dagger\rho_S(t) + \rho_S(t)d_{m'}d_m^\dagger - 2d_m^\dagger\rho_S(t)d_{m'}\right),\end{aligned} \tag{6.10}$$

where

$$\overline{\Omega}_1 = \Omega_1 + A_{+2}^2 A_{+1}^2 P(\Omega_+) + A_{-2}^2 A_{-1}^2 P(\Omega_-) \tag{6.11}$$

$$\overline{\Omega}_2 = \Omega_2 + A_{+2}^4 P(\Omega_+) + A_{-2}^4 P(\Omega_-) \tag{6.12}$$

$$\overline{g} = g + A_{+2}^3 A_{+1} P(\Omega_+) + A_{-2}^3 A_{-1} P(\Omega_-) \tag{6.13}$$

$$K_{mm'}^1 = A_{+2}^2 A_{+m} A_{+m'}\gamma_-(\Omega_+) + A_{-2}^2 A_{-m} A_{-m'}\gamma_-(\Omega_-) \tag{6.14}$$

$$K_{mm'}^2 = A_{+2}^2 A_{+m} A_{+m'}\gamma_+(\Omega_+) + A_{-2}^2 A_{-m} A_{-m'}\gamma_+(\Omega_-) \tag{6.15}$$

$$P(\Omega_\pm) = \int d\omega \frac{J(\omega)}{\Omega_\pm - \omega} \to 0 \tag{6.16}$$

The Lamb-Shift in our model is zero so that the Hamiltonian part is just given by the system Hamiltonian. As equation (6.10) is quite cumbersome we shall only use the quantum master equation in the coupled basis for further discussions.

6.2. Quantum Master Equation in the Local Basis

In this section we derive another master equation in Lindblad form without invoking the secular approximation.

In this section we will make a somewhat different approach and neglect the subsystem interaction in the exponentials transforming an operator to the interaction picture (see Eq. (6.17)). We will, however, retain the interaction term in the Hamiltonian part of the QME.

$$\tilde{O}(t) = e^{iH_S t} O e^{-iH_S t} \approx e^{iH_0 t} O e^{-iH_0 t}, \tag{6.17}$$

where $H_S = H_0 + H_{12} = \Omega_1 d_1^\dagger d_1 + \Omega_2 d_2^\dagger d_2 + g\left(d_1^\dagger d_2 + d_2^\dagger d_1\right)$ as has been defined before. This approximation is for example suggested in [10]. [5, Sect. 6.4] also arrive at this approach by employing a projection operator ansatz and assuming weak intersubsystem coupling ($g \lesssim V$). They refer to [7] where it was found that even for larger g the obtained QME might yield good results under certain conditions.

With approximation (6.17) the interaction picture representation of the creation and annihilation operators in the local basis can easily be calculated as in appendix A.2. Starting from the QME in Born-Markov approximation (cf. Eq (4.32)) we therefore arrive at exactly the same Lindblad terms for the second level coupled to the bath as for the resonant level model in the last chapter. The first system level only enters the Hamiltonian part of the master equation which then reads:

$$\begin{aligned}\frac{d}{dt}\rho_S(t) = &- i\left[\Omega_1 d_1^\dagger d_1 + \Omega_2 d_2^\dagger d_2 + g\left(d_1^\dagger d_2 + d_2^\dagger d_1\right), \rho_S(t)\right] \\ &+ \gamma_-\left(2 d_2 \rho_S(t) d_2^\dagger - d_2^\dagger d_2 \rho_S(t) - \rho_S(t) d_2^\dagger d_2\right) \\ &+ \gamma_+\left(2 d_2^\dagger \rho_S(t) d_2 - d_2 d_2^\dagger \rho_S(t) - \rho_S(t) d_2 d_2^\dagger\right),\end{aligned} \tag{6.18}$$

where we have again introduced

$$\gamma_- = \pi J(\Omega_2)(1 - f(\Omega_2, T)) \tag{6.19}$$

$$\gamma_+ = \pi J(\Omega_2) f(\Omega_2, T), \tag{6.20}$$

where $f(\Omega, T)$ denotes the Fermi-Dirac-function, $J(\Omega)$ the spectral density (which is assumed to be constant) and T the temperature of the bath.

6.3. Comparison

Coupled Basis

First, we derive the steady state for the density matrix in the coupled basis QME (6.9). The QME looks similar to the master equation of the resonant level model with a second level added. The levels in the new basis are not coupled anymore and

are both affected by their respective dissipative terms where the decay constants are proportional to the Fermi-functions of the levels' energies. We write the steady state solution in analogy to the resonant level model as[4]:

$$\rho_{SS} = \begin{pmatrix} f(\Omega_+,T) & 0 \\ 0 & 1-f(\Omega_+,T) \end{pmatrix} \otimes \begin{pmatrix} f(\Omega_-,T) & 0 \\ 0 & 1-f(\Omega_-,T) \end{pmatrix} \tag{6.21}$$

$$= f(\Omega_+)f(\Omega_-)D_+^\dagger D_+ D_-^\dagger D_- + (1-f(\Omega_+))f(\Omega_-)D_+ D_+^\dagger D_-^\dagger D_- \tag{6.22}$$
$$+ f(\Omega_+)(1-f(\Omega_-))D_+^\dagger D_+ D_- D_-^\dagger + (1-f(\Omega_+))(1-f(\Omega_-))D_+ D_+^\dagger D_- D_-^\dagger$$

Note that the steady state is diagonal in the eigenbasis and corresponds to the correct thermal (i.e. Boltzmann) occupation of the system levels with respect to the temperature T of the bath. That this is indeed the steady state can easily be verified by calculation.

Local Basis

Let us now consider the QME (6.18) and determine the occupation number of the levels in the steady state. We therefore consider the equations:

$$\left\langle \dot{N}_1 \right\rangle = 0 \quad \text{and} \quad \left\langle \dot{N}_2 \right\rangle = 0, \tag{6.23}$$

where for a general operator O the time derivative of the expectation value $\left\langle \dot{O} \right\rangle$ is given by:

$$\left\langle \dot{O} \right\rangle = \mathrm{tr}_S(O\dot{\rho}_S) \tag{6.24}$$
$$= \mathrm{tr}_S(O\mathcal{L}\rho) \tag{6.25}$$
$$= -i\mathrm{tr}_S(O\,[H,\rho_S]) + \mathrm{tr}_S(O\mathcal{D}\rho_S) \tag{6.26}$$

Using equation (6.25) we find an inhomogeneous system of coupled differential equations of first order for the occupations and the tunneling-terms:

$$\begin{pmatrix} \left\langle \dot{N}_1 \right\rangle \\ \left\langle \dot{N}_2 \right\rangle \\ \left\langle \dot{d_1^\dagger d_2} \right\rangle \\ \left\langle \dot{d_2^\dagger d_1} \right\rangle \end{pmatrix} = \begin{pmatrix} 0 & 0 & -ig & ig \\ 0 & -2\gamma & ig & -ig \\ -ig & ig & -i\Omega-\gamma & 0 \\ ig & -ig & 0 & i\Omega-\gamma \end{pmatrix} \cdot \begin{pmatrix} \langle N_1 \rangle \\ \langle N_2 \rangle \\ \left\langle d_1^\dagger d_2 \right\rangle \\ \left\langle d_2^\dagger d_1 \right\rangle \end{pmatrix} + \begin{pmatrix} 0 \\ 2\gamma_+ \\ 0 \\ 0 \end{pmatrix} \tag{6.27}$$

where we have introduced $\Omega = \Omega_2 - \Omega_1$ and $\gamma = \gamma_+ + \gamma_- = J\pi$.

In the steady state, the occupation numbers will not change. Also, the hopping-rate will not change. The above equation therefore simplifies to a simple algebraic equation

[4]The tensor product is here with respect to the eigenbasis where the Hilbert space of the system is given by $\mathcal{H} = \mathcal{H}_+ \otimes \mathcal{H}_-$.

where the vector on the left hand side is set equal to zero. We obtain the steady-state expectation values:

$$\langle N_1 \rangle_{SS} = \langle N_2 \rangle_{SS} = \frac{\gamma_+}{\gamma_+ + \gamma_-} = f(\Omega_1, T) \tag{6.28}$$

$$\left\langle d_1^\dagger d_2 \right\rangle_{SS} = \left\langle d_2^\dagger d_1 \right\rangle_{SS} = 0, \tag{6.29}$$

where for the last equality in (6.28) we used the definition of $\gamma_\pm$ (see remark below 6.18).

We obtain a somewhat startling result for the steady state: The occupation number of the first level will be exactly the same as for the second regardless of their respective energies. Also, the correlations between the two levels will be completely destroyed such that no hopping between the two levels will occur. We explain this as follows.

As for the resonant level model discussed in the previous chapter the Lindblad terms in the QME try to drive the second level into its thermal state given by Eq. (5.11). If the coupling to the first level was zero the dynamics would be exactly the same as for the resonant level model with the second level ending up in a mixed state (see dashed line in Fig. 6.2). Choosing a finite coupling will, in general, allow for some tunneling of particles between the two levels. Once an electron occupies the second level, it can, however, not only tunnel to the first level but also to the bath. Due to the effective description of this process via Lindblad drive the Hamiltonian dynamics is disrupted. Part of the occupation of the second level incoherently decays into the bath and is incoherently put back until the second level has been completely driven into its thermal state. A formerly pure state becomes a mixed state. This extraction and insertion is governed by the same process as for the resonant level model and will therefore take place on a timescale $\gamma^{-1} = (\pi V^2 \rho)^{-1}$ (again, cf. dashed line in Fig. 6.2). The tunneling between the two levels occurs on a timescale that is induced by the eigenenergies of the hybridized system as it is similar (at least for short times and weak coupling of the second level to the bath) to the unitary evolution of the free double well potential (cf. oscillations with different frequencies in Fig. 6.2b and 6.2c with respect to 6.2a).

We note that the strength of the current decreases as the levels are detuned with respect to each other. Therefore, the time until the first level reaches its steady state increases (see blue solid line in 6.2c). This is in complete analogy to the only partial transfer of occupation from one level to the other for detuned levels in a unitary evolution. The second level almost purely decays into its thermal state (compare the black dashed and the red solid line in Fig. 6.2c). The occupation of the first level still increases until it reaches the occupancy of the second as for unequal occupations the current operator still yields a finite contribution: Occupation is transported from the fuller (second) to the emptier (first) level. The current does not invert its direction (as would be expected for unitary evolution) due to the incoherent dissipative dynamics acting on the second level which in turn disrupts the correlations between the two levels. The second level is, so to say, constantly "reset" into a mixed state close to its thermal state which allows for current to the first level.

Note that the steady state does not depend on the coupling-strength V so that changing V merely effects the time until the unitary dynamics dies out and the steady state is reached.

As we have seen, equilibrium properties are best described in the coupled basis as the local QME gives the wrong behavior by completely neglecting the effect of the bath on the first level. In the next chapter we will consider the case where a second bath has been introduced which is coupled to the first level. As we will see, neglecting the intersubsystem coupling in the interaction picture is basically a weak-coupling approximation in g and therefore valid as long as the first level is coupled to a bath of its own. If, as is the case for the above model, there is no second bath present we can not neglect the dissipative effects on the first level which are transmitted through the second level as there are no other "stronger" effects present.

6.4. Discussion of the Born-Markov Approximation

We had started the derivation of the QMEs in this chapter by introducing the Born-Markov approximation. In chapter 4 we have justified this approximation for the case of a simple system evolving on a timescale τ_R in the interaction-picture. An example for such a simple system is the resonant level model discussed in the the previous chapter. [8] raise the question whether this approximation is still valid when considering composite systems as there arises a new timescale due to the intersubsystem coupling g.

For the application of the Markov approximation to be valid the existence of two distinct timescales has been crucial: Only when the reduced density matrix varies slowly compared to the timescale τ_B on which the bath correlation functions decay, we can make it local in time. A physical explanation for this is given in [9, Sec. 1.3.3]. There the author argues that the nonlocality in time stems from an imprinting of the system's state onto the environment which then influences the system's future evolution. It is further argued that this effect can, however, be neglected once the memory time in the bath (and hence its correlation time) is short.

We arrived at the Born approximation by making use of projection operator methods. It was found that the factorization of the density matrix for times $t > t_0$ is the result of the small-coupling approximation of the system to the bath which remains valid also for our composite system.

As we have included the intersubsystem coupling in the generator of the interaction picture the reduced density matrix in the interaction picture only evolves due to the coupling to the bath which we assumed to be small. For the derivation in the eigenbasis there do, however, arise fast-oscillating terms. Due to the secular approximation which can be understood as an averaging over the internal coupling time g^{-1} [8] they can be eliminated such that the Markov approximation is valid. Similarly, for the derivation in the local basis the internal coupling is dropped from the generator of the interaction picture such that no fast-oscillating terms arise.

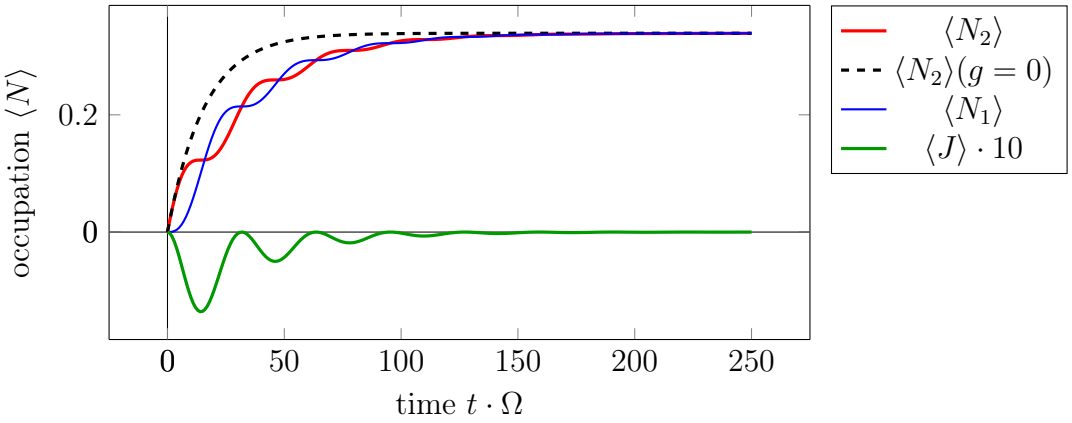

(a) Dynamics for degenerate energies of the two levels $\Omega_1 = \Omega_2 = 2\Omega$.

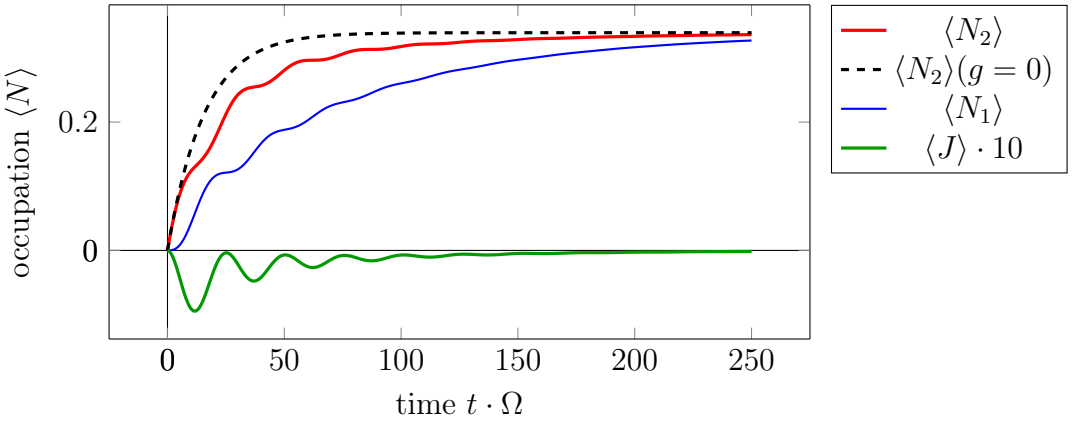

(b) Dynamics for slightly off-resonant energies of the two levels $\Omega_1 = 2.15\Omega, \Omega_2 = 2\Omega$.

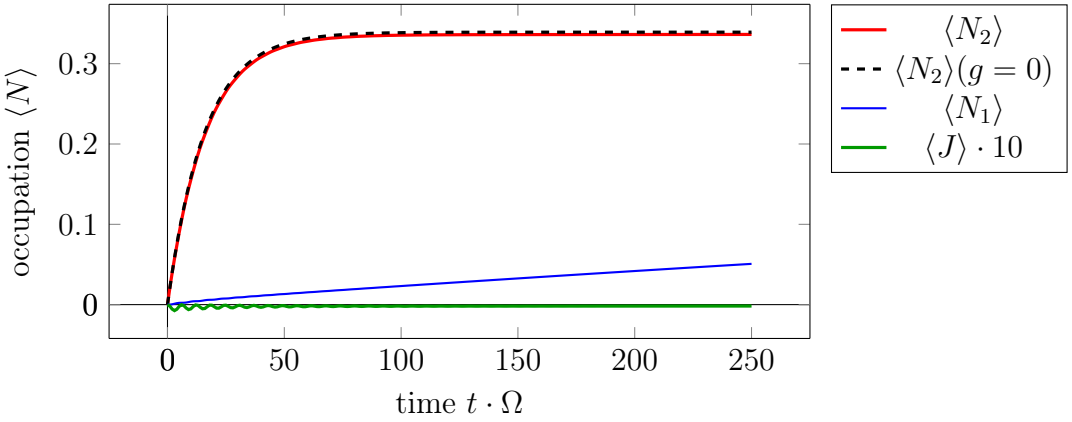

(c) Dynamics for off-resonant energies of the two levels $\Omega_1 = 3\Omega, \Omega_2 = 2\Omega$.

Figure 6.2.: Comparison of the dynamics of the occupation for different values of Ω_1 and Ω_2. The dynamics of a single resonant level (see blue line, $\langle N_2 \rangle (g = 0)$) is compared to the case when the first level is coupled to it. In the steady state both states have the same occupancy. The parameters used are: $g = 0.1\Omega, V = 0.1\Omega, T = 3\Omega, \rho_{\text{bath}} = 1/\Omega, \rho(t = 0) = |00\rangle \langle 00|$, where we have introduced the energy scale Ω and density of states in the bath ρ_{bath}.

7. Two Coupled Levels with two Taths

We now consider a model with two levels coupled to each other and to two baths with temperatures T_1 and T_2 respectively. A schematic representation is depicted in Fig. 7.1 and the entire Hamiltonian is given by Eq. (7.1):

$$H = H_S + H_{B1} + H_{B2} + H_{I1} + H_{I2}, \tag{7.1}$$

where the different parts of the Hamiltonian are given by:

$$\begin{aligned} H_S &= \begin{pmatrix} d_1^\dagger & d_2^\dagger \end{pmatrix} \begin{pmatrix} \Omega_1 & g \\ g & \Omega_2 \end{pmatrix} \begin{pmatrix} d_1 & d_2 \end{pmatrix} \\ H_{Bi} &= \sum_q \omega_{iq} c_{iq}^\dagger c_{iq} \quad (i \in \{1,2\}) \\ H_{Ii} &= V_i \sum_q \left(d_i^\dagger c_{iq} + c_{iq}^\dagger d_i \right) \end{aligned} \tag{7.2}$$

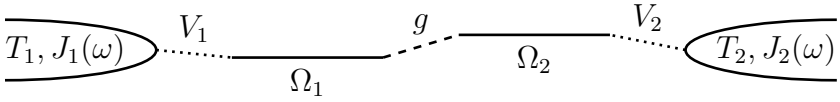

Figure 7.1.: Schematic depiction of two levels coupled to two baths. All the bath modes are combined to a bath with temperature T_i and spectral density $J_i(\omega)$

As before we want to find an appropriate QME (in Lindblad form) that describes the dynamics of the system. We have seen in the last chapter that working in the eigenbasis of the hybridized system yields a QME that describes the steady state correctly. For the model considered in this section we can also discuss nonequilibrium properties such as steady state particle current which arises, for example, from different bath temperatures $T_1 \neq T_2$. Again we have to introduce a secular approximation in order to arrive at an equation that is in Lindblad form. We will see that this QME then always yields a vanishing particle current in the steady state independent of the bath temperatures.

We therefore also consider the QME in the local basis (although it does not yield the correct steady state occupation number) which yields a finite current in the steady state. We will compare this to the correct current which can be obtained exactly using Keldysh formalism.

7.1. Exact Current using Keldysh Formalism

In this section we quote an expression for the current in the steady state (for the model given above) that is outlined and derived in [1, Chap. 12] by means of Keldysh formalism. It is beyond the scope of this Bachelor thesis to derive it or explain the underlying formalism. The current J is related to the transmission probability $T(\epsilon)$ via the equation

$$J = \frac{e}{\hbar}\int \frac{d\epsilon}{2\pi} T(\epsilon)\left[f_L(\epsilon) - f_R(\epsilon)\right], \tag{7.3}$$

where $T(\epsilon)$ is given by

$$T(\epsilon) = \mathrm{tr}\{\mathbf{\Gamma}^L(\epsilon)\mathbf{G}^r(\epsilon)\mathbf{\Gamma}^R(\epsilon)\mathbf{G}^a(\epsilon)\}, \tag{7.4}$$

and f_L and f_R denote the Fermi-Dirac-distribution for the left and right bath respectively.

The Dyson equation for $\mathbf{G}^{r/a}(\epsilon)$ is given by:

$$\mathbf{G}^{r/a}(\epsilon) = \mathbf{g}^{r/a}(\epsilon) + \mathbf{g}^{r/a}(\epsilon)\mathbf{\Sigma}^{r/a}(\epsilon)\mathbf{G}^{r/a}(\epsilon) \tag{7.5}$$

from which we find by matrix inversion:

$$(\mathbf{G}^{r/a}(\epsilon))^{-1} = (\mathbf{g}^{r/a}(\epsilon))^{-1} - \mathbf{\Sigma}^{r/a}(\epsilon), \tag{7.6}$$

where $\mathbf{g}^{r/a}(\epsilon)$ is given by (with η infinitesimally positive)

$$(\mathbf{g}^{r/a}(\epsilon))^{-1} = \epsilon - H \pm i\eta. \tag{7.7}$$

The tunneling self-energy $\mathbf{\Sigma} = \mathbf{\Sigma}_R + \mathbf{\Sigma}_L$ is given by ($\alpha \in \{R, L\}$)

$$\Sigma^{r/a}_{\alpha,mn}(\epsilon) = \sum_k V^*_{\alpha k,m} g^{r/a}_{\alpha k}(\epsilon) V_{\alpha k,n} = \Lambda^\alpha_{mn}(\epsilon) \mp \frac{i}{2}\Gamma^\alpha_{mn}(\epsilon) \tag{7.8}$$

with

$$g^{r/a}_k(\epsilon) = \lim_{\eta\to 0^+} \frac{1}{\epsilon - \epsilon_k \pm i\eta} \tag{7.9}$$

and level-width function $\mathbf{\Gamma} = \mathbf{\Gamma}^L + \mathbf{\Gamma}^R$ which is defined by ($\alpha \in \{R, L\}$):

$$(\Gamma^\alpha(\epsilon_k))_{mn} = 2\pi\rho_\alpha(\epsilon_k) V_{\alpha,n}(\epsilon_k) V^*_{\alpha,m}(\epsilon_k). \tag{7.10}$$

Using the above definitions we therefore find for our model

$$\mathbf{\Sigma}^{r/a}(\epsilon) \equiv \mathbf{\Sigma}^{r/a} = \begin{pmatrix} \mp i\pi V^2\rho & 0 \\ 0 & \mp i\pi V^2\rho \end{pmatrix} = \mp\frac{i}{2}\mathbf{\Gamma} \tag{7.11}$$

$$\mathbf{\Gamma}^L = 2\pi\rho V^2 \begin{pmatrix} 1 & 0 \\ 0 & 0 \end{pmatrix} \equiv \Gamma^L \begin{pmatrix} 1 & 0 \\ 0 & 0 \end{pmatrix} \quad \text{and} \quad \mathbf{\Gamma}^R = 2\pi\rho V^2 \begin{pmatrix} 0 & 0 \\ 0 & 1 \end{pmatrix} \equiv \Gamma^R \begin{pmatrix} 0 & 0 \\ 0 & 1 \end{pmatrix} \tag{7.12}$$

This yields

$$\mathbf{G}^{r/a}(\omega) = \begin{pmatrix} \omega - \Omega_1 - \Sigma_{11}^{r/a} & -g \\ -g & \omega - \Omega_2 - \Sigma_{22}^{r/a} \end{pmatrix}^{-1} \tag{7.13}$$

which finally leads to the following expression for the particle current:

$$J = \frac{e}{\hbar} \int \frac{d\omega}{2\pi} \Gamma^L \Gamma^R G_{12}^r(\omega) G_{21}^a(\omega) [f_L(\omega) - f_R(\omega)] \tag{7.14}$$

Using these explicit expressions (7.11) to (7.13) we can calculate the prefactor in front of the difference of the Fermi functions a plot of which can be found in Fig. 7.2:

$$\frac{1}{2\pi} \frac{4g^2\pi^2\rho^2V^4}{(g^2 - (\omega - \Omega_1)(\omega - \Omega_2))^2 + (2g^2 + 2\omega^2 + \Omega_1^2 + \Omega_2^2 - 2\omega(\Omega_1 + \Omega_2))\pi^2\rho^2V^4 + \pi^4\rho^4V^8)} \tag{7.15}$$

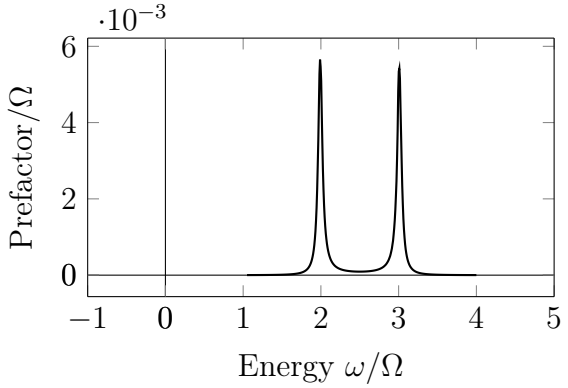

Figure 7.2.: Plot of the prefactor of the difference of the Fermi functions in equation (7.14). The parameters used are $\Omega_1 = 3\Omega, \Omega_2 = 2\Omega, g = 0.1\Omega, V = 0.1\Omega$, $\rho = 1\Omega^{-1}$, where we have introduced the energy scale Ω.

The function falls of to zero for large energies and has two distinct maxima whose width is determined by the parameter V. The maxima are at the following positions:

$$\omega_{\max,1/2} = \frac{\Omega_1 + \Omega_2}{2} \pm \frac{1}{2}\sqrt{4g^2 + (\Omega_1 - \Omega_2)^2 - 4\pi^2V^4)} \tag{7.16}$$

This yields the following height of the peaks in Fig 7.2:

$$\text{height}(\omega_{\max,1/2}) = \frac{1}{2\pi} \frac{4g^2}{4g^2 + (\Omega_1 - \Omega_2)^2}. \tag{7.17}$$

The width of these peaks is proportional to ρV^2 so that we can very roughly estimate the current to be[1]:

$$J \propto \rho V^2 \frac{1}{2\pi} \frac{4g^2}{4g^2 + (\Omega_1 - \Omega_2)^2} (f_L(\omega_{\max,1}) - f_R(\omega_{\max,1}) + f_L(\omega_{\max,2}) - f_R(\omega_{\max,2})) \tag{7.18}$$

[1] We assume that the width of the peaks is much smaller than their distance and the Fermi function does not change much in one peak.

The integral involved in calculating the exact current (7.14) can, however, not be evaluated analytically so that we have to defer to numerical integration. This is done in the Sec. 7.4 using the function `quadgk` built in to `matlab` which allows for an infinite range of integration.

In the following we will again give derivations for two different QME in Lindblad form. As has been noted in [7] our derivations correspond to a strong coupling approximation (derivation in the eigenbasis) and a weak coupling approximation (derivation in the local basis). Weak and strong refer to the strength of the intersubsystem coupling with respect to the coupling to the baths.

7.2. QME in the Eigenbasis

Using a similar projection operator method as before (for a detailed derivation see [7, Appendix B.2]) it was found that the QME in Born-approximation for the reduced density matrix gives separate Lindblad terms for the two baths. Assuming Markovian dynamics we arrive at the QME in Born-Markov-approximation in the interaction picture:

$$\begin{aligned}\frac{d}{dt}\tilde{\rho}_S(t) = -\int_0^\infty ds \Big\{ &\mathrm{tr}_{B_1}\left[\tilde{H}_{I1}(t), \left[\tilde{H}_{I1}(t-s), \tilde{\rho}_S(t)\otimes\rho_{th1}\right]\right] \\ &+ \mathrm{tr}_{B_2}\left[\tilde{H}_{I2}(t), \left[\tilde{H}_{I2}(t-s), \tilde{\rho}_S(t)\otimes\rho_{th2}\right]\right]\Big\}\end{aligned} \tag{7.19}$$

Note, that there do not appear any crossterms between H_{I1} and H_{I2} as can be seen from the detailed derivation. Due to this we can calculate the two contributions to the QME separately. Following the steps from chapter 6 we diagonalize the system and express the system-bath-couplings in terms of the new creation and annihilation operators of the coupled basis (cf. appendix A.7). There, the interaction Hamiltonian reads as follows:

$$H_{Ij} = \underbrace{\sum_{n=\pm}\left(A_{nj}D_n^\dagger\right)}_{\mathrm{S_{1j}}} \otimes \underbrace{V_j \sum_q c_{qj}}_{\mathrm{B_{1j}}} + \underbrace{V_j \sum_q c_{qj}^\dagger}_{\mathrm{B_{2j}}} \otimes \underbrace{\sum_{n=\pm}\left(A_{nj}D_n\right)}_{\mathrm{S_{2j}}} \tag{7.20}$$

As the contributions from the different baths can be calculated separately (see above) we arrive at two expressions that are similar to Eq.(6.5) so that we will merely copy the results obtained before. For the contribution of the first bath we obtain[2]:

$$\begin{aligned}\mathcal{D}_1\tilde{\rho}_S(t) = -\sum_{n=\pm} A_{n1}^2 \Big\{ &\left(\gamma_-(\Omega_{n'}) + i\Delta_-(\Omega_{n'})\right) e^{i(\Omega_n-\Omega_{n'})t}\left(D_n^\dagger D_{n'}\tilde{\rho}_s(t) - D_{n'}\tilde{\rho}_s(t)D_n^\dagger\right) \\ &+ \left(\gamma_+(\Omega_{n'}) + i\Delta_+(\Omega_{n'})\right) e^{i(\Omega_{n'}-\Omega_n)t}\left(D_n D_{n'}^\dagger\tilde{\rho}_s(t) - D_{n'}^\dagger\tilde{\rho}_s(t)D_n\right) \\ &+ \mathrm{h.c.}\Big\}\end{aligned} \tag{7.21}$$

[2] We will skip the index 1 indicating "contribution of the first bath"

A similar contribution arises for the second bath. Note that the γ- and Δ-functions introduced in Eq. (6.7) will now depend on the respective temperatures of the corresponding bath.

As before we have to introduce a secular approximation in order to arrive at a Lindblad-equation. Neglecting the fast-rotating terms (cf. the discussion above Eq. (6.8)) we can drop one index of the double-sum and are left with (after going back to the Schrödinger picture) the Lindblad master equation for the entire system[3]:

$$\begin{aligned}\frac{d}{dt}\rho_S = -i[H_S,\rho_S] &+ \sum_{n=\pm}\left(\gamma_-^{(1,n)}A_{n1}^2 + \gamma_-^{(2,n)}A_{n2}^2\right)\left(2D_n\rho_S D_n^\dagger - D_n^\dagger D_n\rho_S - \rho_S D_n^\dagger D_n\right)\\ &+ \sum_{n=\pm}\left(\gamma_+^{(1,n)}A_{n1}^2 + \gamma_+^{(2,n)}A_{n2}^2\right)\left(2D_n^\dagger\rho_S D_n - D_nD_n^\dagger\rho_S - \rho_S D_nD_n^\dagger\right),\end{aligned} \tag{7.22}$$

where we have again introduced

$$\gamma_-^{(i,n)} = \pi J_i(\Omega_n)(1-f(\Omega_n,T_i)) \tag{7.23}$$

$$\gamma_+^{(i,n)} = \pi J_i(\Omega_n)f(\Omega_n,T_i) \tag{7.24}$$

and have used the fact that the Lamb Shift vanishes for our model (cf. Eq. (5.8)).

For further use we rewrite the decay-constants of the dissipative terms using the relation between A_{n1} and A_{n2} (cf. equation (A.46)),

$$A_{n1}^2 + A_{n2}^2 = 1,$$

and assuming that the spectral density J is independent of temperature. This is possible for constant density of states and equal baths. We thus arrive at:

$$\begin{aligned}\gamma_+^{(1)}(\Omega_n)A_{n1}^2 + \gamma_+^{(2)}(\Omega_n)A_{n2}^2 &= \pi J(\Omega_n)\left\{f(\Omega_n,T_1) + A_{n2}^2\left[f(\Omega_n,T_2)-f(\Omega_n,T_1)\right]\right\}\\ &\equiv \pi J(\Omega_n)x_n\end{aligned} \tag{7.25}$$

$$\begin{aligned}\gamma_-^{(1)}(\Omega_n)A_{n1}^2 + \gamma_-^{(2)}(\Omega_n)A_{n2}^2 &= \pi J(\Omega_n)\left\{1-f(\Omega_n,T_1) - A_{n2}^2\left[f(\Omega_n,T_2)-f(\Omega_n,T_1)\right]\right\}\\ &= \pi J(\Omega_n) - \left[\gamma_+^{(1)}(\Omega_n)A_{n1}^2 + \gamma_+^{(2)}(\Omega_n)A_{n2}^2\right]\\ &\propto 1 - \left\{f(\Omega_n,T_1) + A_{n2}^2\left[f(\Omega_n,T_2)-f(\Omega_n,T_1)\right]\right\}\\ &\equiv \pi J(\Omega_n)(1-x_n)\end{aligned} \tag{7.26}$$

For the case of equal bath temperatures $T_1 = T_2 = T$ this can be simplified further to yield:

$$\gamma_+^{(1)}(\Omega_n)A_{n1}^2 + \gamma_+^{(2)}(\Omega_n)A_{n2}^2 = \pi J(\Omega_n)f(\Omega_n,T) \tag{7.27}$$

$$\gamma_-^{(1)}(\Omega_n)A_{n1}^2 + \gamma_-^{(2)}(\Omega_n)A_{n2}^2 = \pi J(\Omega_n)\left[1-f(\Omega_n,T)\right]. \tag{7.28}$$

[3]We have dropped the time-argument of the reduced density matrix in order to simplify notation.

7.3. QME in the Local Basis

Again we will also derive a master equation in the local basis. As in the last section the derivation of the two levels can be done separately and in complete analogy to our previous calculations (starting with the QME in Born-Markov approximation from [7, Appendix B.1] which implies approximation (6.17) as before). The master equation we finally obtain is the following[4]:

$$\begin{aligned}\frac{d}{dt}\rho_S = -i\left[H_S, \rho_S\right] + \sum_{i=1,2} \gamma_-^{(i)}(\Omega_i)\left(2d_i\rho_S d_i^\dagger - d_i^\dagger d_i\rho_S - \rho_S d_i^\dagger d_i\right) \\ + \gamma_+^{(i)}(\Omega_i)\left(2d_i^\dagger\rho_S d_i - d_i d_i^\dagger\rho_S - \rho_S d_i d_i^\dagger,\right)\end{aligned} \tag{7.29}$$

where the $\gamma_\pm^{(i)}(\Omega_i)$ are defined as above but with $i \in \{1,2\}$ rather than $\{+,-\}$:

$$\gamma_-^{(i)} = \pi J(\Omega_i)(1 - f(\Omega_i, T_i)) \tag{7.30}$$

$$\gamma_+^{(i)} = \pi J(\Omega_i) f(\Omega_i, T_i) \tag{7.31}$$

7.4. Comparison

Coupled Basis

For the coupled basis it is again easy to write down the steady-state solution as the Hamiltonian is that of two uncoupled levels. Making use of the special form of the decay constants (see Eq. (7.25) and (7.26)) the steady-state can be written as[5]:

$$\rho_{SS} = \begin{pmatrix} x_+ & 0 \\ 0 & 1-x_+ \end{pmatrix} \otimes \begin{pmatrix} x_- & 0 \\ 0 & 1-x_- \end{pmatrix} \tag{7.32}$$

$$\begin{aligned}&= x_+x_-D_+^\dagger D_+ D_-^\dagger D_- + (1-x_+)x_- D_+ D_+^\dagger D_-^\dagger D_- \\ &\quad + x_+(1-x_-)D_+^\dagger D_+ D_- D_-^\dagger + (1-x_+)(1-x_-)D_+ D_+^\dagger D_- D_-^\dagger\end{aligned} \tag{7.33}$$

where $x_\pm = f(\Omega_\pm, T_1) + A_{\pm 2}^2\left[f(\Omega_\pm, T_2) - f(\Omega_\pm, T_1)\right]$. Note that $\mathrm{tr}(\rho_{SS}) = 1$ and that $\frac{d}{dt}\rho_{SS} = 0$ can be verified by simple calculation.

For the case of equal bath temperatures the steady state is by construction the thermal state of the system (including the coupling) with respect to the joint bath temperature. We also note that in the steady state there will be no current. This can be seen by the following argument: In order for the expectation value of the current operator[6]

$$J = \frac{g}{i}\left(d_2^\dagger d_1 - d_1^\dagger d_2\right) \tag{7.34}$$

[4] again we drop the time argument of $\rho_S(t)$

[5] The tensor product is here with respect to the eigenbasis where the Hilbert space of the system is given by $\mathcal{H} = \mathcal{H}_+ \otimes \mathcal{H}_-$.

[6] For a derivation of the current operator refer to appendix A.8.1

to attain a non-zero value, the density matrix of the system needs to have complex entries as all real contributions will be canceled due to the sign in the current operator and the hermicity condition of the density matrix. The steady state given above is, however, real valued so that it yields a vanishing net particle current between the two levels. A similar result has been found for the energy current in a spin-chain [10] where the authors attribute the vanishing energy current to the diagonal form of the steady state density matrix in the energy eigenbasis after invoking a secular approximation. As there, we find that the QME in the secular approximation is inappropriate to describe non-equilibrium dynamics.

Local Basis

For the QME in the local basis the steady state can be derived exactly as for the system with just one bath (cf. Sec. 6.3). Following the same procedure we arrive at the following differential equation for the expectation values:

$$\begin{pmatrix} \dot{\langle N_1 \rangle} \\ \dot{\langle N_2 \rangle} \\ \dot{\langle d_1^\dagger d_2 \rangle} \\ \dot{\langle d_2^\dagger d_1 \rangle} \end{pmatrix} = \begin{pmatrix} -2\gamma^{(1)} & 0 & -ig & ig \\ 0 & -2\gamma^{(2)} & ig & -ig \\ -ig & ig & -i\Omega - \gamma & 0 \\ ig & -ig & 0 & i\Omega - \gamma \end{pmatrix} \cdot \begin{pmatrix} \langle N_1 \rangle \\ \langle N_2 \rangle \\ \langle d_1^\dagger d_2 \rangle \\ \langle d_2^\dagger d_1 \rangle \end{pmatrix} + \begin{pmatrix} 2\gamma_+^{(1)} \\ 2\gamma_+^{(2)} \\ 0 \\ 0 \end{pmatrix} \tag{7.35}$$

where we have introduced $\gamma = (\gamma^{(1)} + \gamma^{(2)})$ and $\gamma^{(i)} = \gamma_+^{(i)} + \gamma_-^{(i)}$ and $\Omega = \Omega_2 - \Omega_1$.

Solving the equation for the steady state using Mathematica we obtain[7]:

$$\langle N_1 \rangle_{SS} = \frac{2f(\Omega_2, T_2)g^2 + f(\Omega_1, T_1)(2g^2 + 4(\pi J)^2 + (\Omega_2 - \Omega_1)^2)}{4(g^2 + (\pi J)^2) + (\Omega_2 - \Omega_1)^2} \tag{7.36}$$

$$\langle N_2 \rangle_{SS} = \frac{2f(\Omega_1, T_1)g^2 + f(\Omega_2, T_2)(2g^2 + 4(\pi J)^2 + (\Omega_2 - \Omega_1)^2)}{4(g^2 + (\pi J)^2) + (\Omega_2 - \Omega_1)^2} \tag{7.37}$$

$$\left\langle d_1^\dagger d_2 \right\rangle_{SS} = \frac{g[f(\Omega_2, T_2) - f(\Omega_1, T_1)](\Omega_2 - \Omega_1 + 2i\pi J)}{4g^2 + 4\pi^2 J^2 + (\Omega_2 - \Omega_1)^2} \tag{7.38}$$

$$\left\langle d_2^\dagger d_1 \right\rangle_{SS} = \frac{g[f(\Omega_2, T_2) - f(\Omega_1, T_1)](\Omega_2 - \Omega_1 - 2i\pi J)}{4g^2 + 4\pi^2 J^2 + (\Omega_2 - \Omega_1)^2} \tag{7.39}$$

We first note that the correlations both depend on the difference of the Fermi functions evaluated at the respective energies and temperatures and do not, in general, vanish as has been the case for the previous model. This can be understood as follows: The newly introduced bath tries to drive its level into the mixed thermal state according to its temperature T_1. Without the coupling between the two levels the steady state would just be the product state of the two respective thermal states:

$$\begin{pmatrix} f_1 & 0 \\ 0 & 1 - f_1 \end{pmatrix} \otimes \begin{pmatrix} f_2 & 0 \\ 0 & 1 - f_2 \end{pmatrix} \tag{7.40}$$

[7] We again assume that the spectral densities are the same for both baths. This leads to $\gamma^{(1)} = \gamma^{(2)} = \pi J$

For $f_1 \neq f_2$ this state yields a finite contribution for the coupling term in the Hamiltonian part of the QME (7.29) which gives rise to complex-valued off-diagonal terms in the density matrix. These terms yield finite expectation values for the coherences (7.38) and (7.39) and the current operator. To summarize, the dissipative terms drive the system towards a diagonal state whereas the Hamiltonian term counteracts this and produces complex off-diagonal terms. In the steady state these two actions equilibrate. For the previous case of just one bath the Hamiltonian part of the QME yields no contribution in the thermal state so that the system ends up there.

Let us also note that, due to the hybridization in the Hamiltonian part of the master equation, the steady state is not the product state of the thermal states as the occupation of the left level does depend on the occupation of the right level and vice versa (see Eq. (7.37))[8]. Due to the form of the dissipative terms the occupations are, however, also not the thermal state occupations of the system one would expect for an equation taking into account the coupling properly (i.e. also in the dissipative terms such as the QME in the eigenbasis).

Let us now turn to the comparison of the particle current between our QME and the exact formula obtained from Keldysh formalism and start by stating the exact results.

For equal bath temperatures $T_1 = T_2$ a vanishing particle current is obtained as the difference of the Fermi-function in Eq. (7.3) is then always zero. When increasing the temperature of the left bath the difference of the Fermi functions is, in general, not zero. An example is plotted in Fig. 7.3.

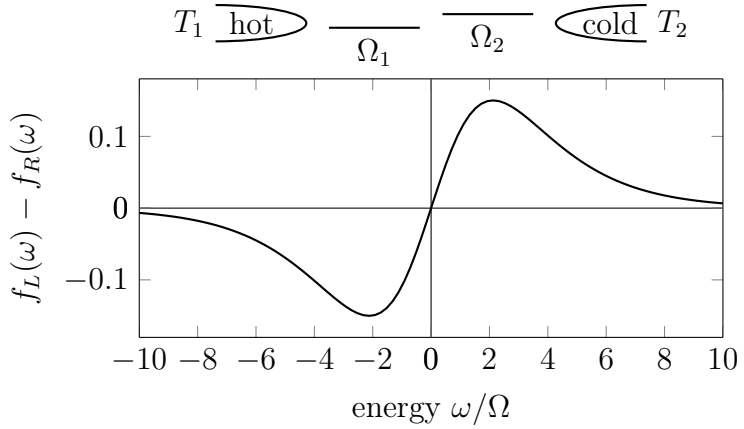

Figure 7.3.: Difference of the two Fermi-functions in Eq. (7.3) with respect to the energy ω.
The parameters used are $T_1 = 2\Omega, T_2 = 1\Omega$, where we have again introduced the energy scale Ω

As we can see from equations (7.3) and (7.14) both, magnitude and direction of the current, will also depend on the energy-dependent prefactor plotted in Fig. 7.2. For

[8] If we take the limit of vanishing coupling, $g \to 0$, we obtain the thermal product state (7.40)

the case depicted in Fig. 7.3 the current flows towards the left when the prefactor's contribution is larger for negative energies, and towards the right if its contribution is larger for positive energies. The first is for example the case for negative Ω_1 and Ω_2, while the latter happens for positive Ω_i (also cf. Eq. (7.16)).

Let us now turn to the results of our QME and its simulation. Evaluating Eq. (7.34) using the above expectation values in the steady state, we find:

$$\frac{g}{i}\left\langle d_2^\dagger d_1 - d_1^\dagger d_2 \right\rangle_{SS} = g^2 J\pi \frac{4\left[f(\Omega_1, T_1) - f(\Omega_2, T_2)\right]}{4g^2 + 4\pi^2 J^2 + (\Omega_2 - \Omega_1)^2} \tag{7.41}$$

This expression looks very similar to the expression we had found when roughly estimating the current from the exact result in Eq. (7.18). However, there the Fermi functions were evaluated at the shifted peak positions $\omega_{\max,1/2}$ rather than $\Omega_{1/2}$ as we have found it here for Eq. (7.41). This, as will also be discussed below, is assumed to be a consequence of the approximation we have introduced before.

We also see that the particle current does not directly depend on the temperatures of the baths but on the respective ratios Ω_1/T_1 and Ω_2/T_2 at which the Fermi functions are evaluated. This has drastic consequences which we summarize for the case[9] $\Omega_1, \Omega_2 \geq 0$ and $T_1 > T_2$ (see cartoon[10] in Fig. 7.4).

	$\frac{\Omega_2}{T_2} < \frac{\Omega_1}{T_1}$	$\frac{\Omega_2}{T_2} = \frac{\Omega_1}{T_1}$	$\frac{\Omega_2}{T_2} > \frac{\Omega_1}{T_1}$
exact	$\longrightarrow$	$\longrightarrow$	$\longrightarrow$
simulation	$\longleftarrow$	0	$\longrightarrow$

Table 7.1.: Direction of the current

In Tab. 7.1 we give the direction of the current for the three possible regimes of Ω_2/T_2. We see that only in the regime $\frac{\Omega_2}{T_2} > \frac{\Omega_1}{T_1} \Leftrightarrow \frac{T_1}{T_2} > \frac{\Omega_1}{\Omega_2}$ the QME yields the correct direction of the current (and therefore the same qualitative behavior). We attribute this to approximation (6.17) that we have introduced in order to arrive at the QME in Lindblad form. Due to neglecting the intersubsystem coupling for the generator of the interaction picture, the two Lindblad drives only "see" the level they are directly coupled to and do not affect the other one. Their insertion and extraction of particles therefore only depends on the occupation of that level and not on the state of the system as a whole. In order to obtain a qualitatively better QME a different approximation scheme would have to be introduced. From a more quantitative analysis (cf. Fig. 7.4) we see that even though it yields the wrong direction for $\frac{\Omega_2}{T_2} < \frac{\Omega_1}{T_1}$, it is only slightly negative.

This being "slightly wrong" is determined by the strength of the coupling g with respect to the energies of the levels Ω_i (cf. also Eq. (7.41)). The coupling strength to the baths V merely determines the magnitude of the current as a whole. The relative error (form of the plots) stays, however, roughly the same.

[9] The other cases can be discussed analogously.

[10] In the following we illustrate the considered situations in little cartoons where dashed arrows will indicate continuous change of a quantity whereas colors will indicate different discrete values.

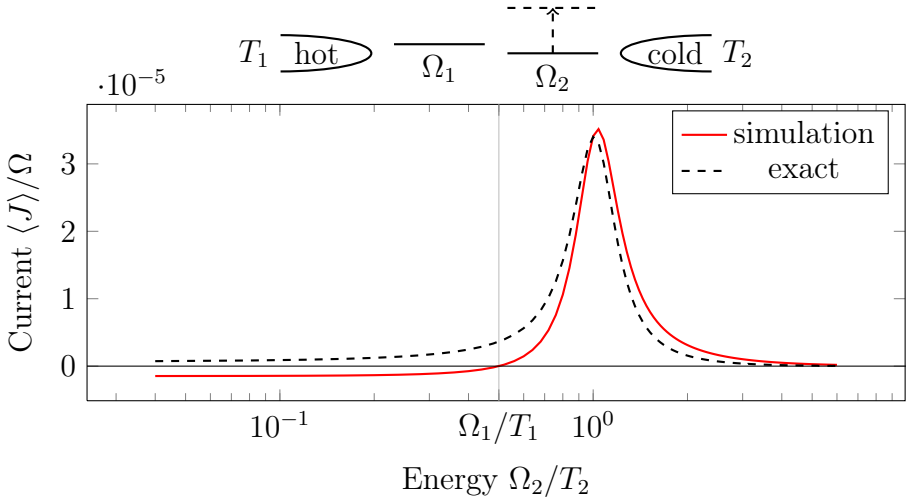

Figure 7.4.: Current from the left to the right level with respect to the energy of the second level (see cartoon). The parameters used are: $g = 0.1\Omega, V = 0.01\Omega, \Omega_1 = 1\Omega, T_1 = 2\Omega, T_2 = 1\Omega$

From Fig. 7.4 we see that the simulation yields the same result as the exact formula for $\Omega_2 = \Omega_1$. For this situation it is clear that the QME will always at least get the direction correct as for $T_1 = T_2$ the QME will also yield a vanishing current, and for $T_\alpha > T_\beta$ the current will flow from α to β (for $\Omega_\alpha > 0$, else from β to α).

In Fig. 7.5 we present evidence that for $\Omega_1 = \Omega_2$ the QME yields very good results as long as $g \ll T_2$.

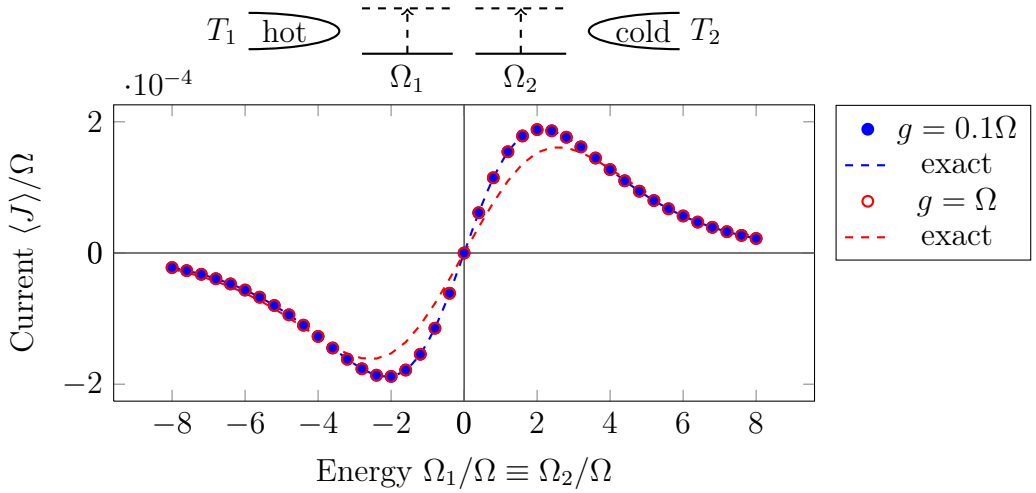

Figure 7.5.: Current from the left to the right level with respect to the energy of the second level (see cartoon).
The parameters used are: $V = 0.02\Omega, T_1 = 2\Omega, T_2 = 1\Omega$

For non-resonant energies the agreement between exact and simulated result is not so good as we have seen in Fig. 7.4 and only qualitatively correct for $\frac{\Omega_2}{T_2} > \frac{\Omega_1}{T_1}$. In Fig. 7.6 we show how the current changes when we change the temperature of the first bath.

Note that from the exact results the current always vanishes for $T_1 = T_2$. We find that for degenerate energies of the levels (blue dots) the simulation and the exact result agree perfectly whereas for off-resonant energies (red and black dots) the agreement is again qualitatively correct for $\frac{\Omega_2}{T_2} > \frac{\Omega_1}{T_1}$. For off-resonant energies the amplitude of the current is also much smaller than for the resonant case.

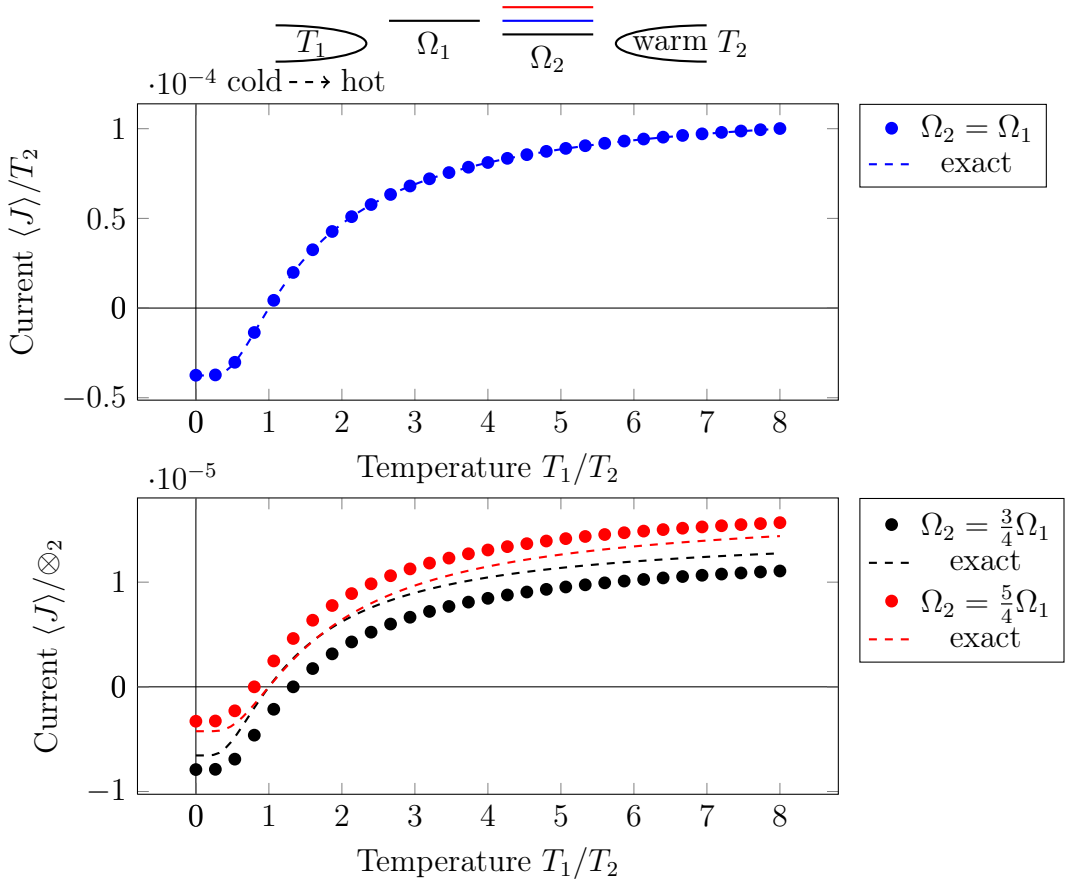

Figure 7.6.: Current from the left to the right level with respect to the temperature of the first bath for three different values of Ω_2 (see cartoon).
The parameters used are: $V = 0.01T_2, g = 0.1T_2, \Omega_1 = 2T_2, T_2 = 1$. T_2 is varied from 0 to $8T_2$.

8. Aharanov-Bohm like Problems

In this chapter we will analyze how the Lindblad terms effect phase coherence. For this we consider a system of four levels coupled to each other and to two baths. The geometry is shown in Fig. 8.1 and we will denote the levels by left, right, first and second. The coupling constants between the levels are chosen to be equal with the exception indicated in the figure where an additional phase factor is acquired when tunneling from the left to the first level. As this looks similar to the system considered by Aharanov and Bohm (cf. [11]) we shall call our model accordingly.

The Hamiltonian is given by:

$$H = H_S + H_{B1} + H_{B2} + H_{I1} + H_{I2} \tag{8.1}$$

$$\begin{aligned} H_S &= \sum_{j=1,2,L,R} \Omega_j d_j^\dagger d_j + \left[g \left(e^{i\phi} d_L^\dagger d_1 + d_L^\dagger d_2 + d_R^\dagger d_1 + d_R^\dagger d_2 \right) + \text{h.c.} \right] \\ H_{Bi} &= \sum_q \omega_{iq} c_{iq}^\dagger c_{iq} \quad (i \in \{1,2\}) \\ H_{Ii} &= V_i \sum_q \left(d_i^\dagger c_{iq} + c_{iq}^\dagger d_i \right) \end{aligned} \tag{8.2}$$

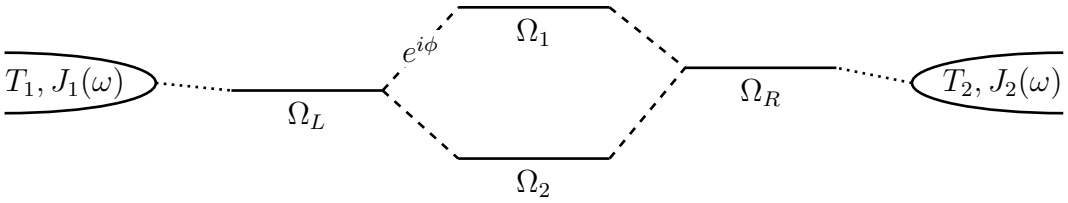

Figure 8.1.: Schematic depiction of the Aharanov-Bohm ring. The coupling constants between the levels are the same except for the coupling between Ω_L and Ω_1 for which an additional phase is acquired. All the bath modes are combined to a bath with temperature T_i and spectral density $J_i(\omega)$

8.1. Unitary Evolution without Coupling to External Baths

We will first consider the unitary evolution of the closed system without coupling to an external bath. Let us put an electron in the left level and set $\phi = 0$. It will tunnel to the first and second level, with the amplitudes depending on the respective energies. From there it will either tunnel to the right level or back to the left. We therefore expect an oscillation of the electron through the system where the occupation probability is again determined by the relative energies of the four levels.

If we now change ϕ to a non-zero value and choose $\Omega_1 = \Omega_2$ we expect interference effects to change the average occupation of the rightmost level. For $\phi = \pi$ we expect destructive interference such that the right level will always be unoccupied: there will not be any net current onto the right level. Tuning the ratio between Ω_1 and Ω_2 away from unity we expect only partial occurance of destructive interference such that the occupation of the right level will return, even for $\phi = \pi$. For the case of non-degenerate system energies, the occupation varies between zero and a maximal value which is determined by the energy of the rightmost level and the phase ϕ. All our expectations can be met by numerical simulations. Figures 8.3 and 8.2 present two examples for the current onto or from the rightmost level which was initially empty. The current operator is in this case given by Eq. (8.3) a derivation of which can be found in appendix A.8.2.

$$\frac{d}{dt}N_R = \frac{g}{i}\left(d_R^\dagger d_1 - d_1^\dagger d_R + d_R^\dagger d_2 - d_2^\dagger d_R\right) \tag{8.3}$$

8.2. QME in the Local Basis

As we have seen the Lindblad master equation derived in the eigenbasis of the system by use of the Secular Approximation yields a vanishing particle current and is therefore inappropriate to describe the problem we consider. We will therefore use the master equation in the local basis. For each level coupled to a bath we obtain, as for the resonant level model, two dissipative terms whereas the other levels and the intersubsystem coupling only occur in the Hamiltonian part of the master equation. As the phase factor is part of the Hamiltonian we expect the existence of a coherent current that will be effected by interference effects.

The QME is given by[1]:

$$\begin{aligned}\frac{d}{dt}\rho_S = -i\left[H_S, \rho_S\right] + \sum_{i=L,R} &\gamma_-^{(i)}(\Omega_i)\left(2d_i\rho_S d_i^\dagger - d_i^\dagger d_i\rho_S - \rho_S d_i^\dagger d_i\right) \\ &+ \gamma_+^{(i)}(\Omega_i)\left(2d_i^\dagger\rho_S d_i - d_i d_i^\dagger\rho_S - \rho_S d_i d_i^\dagger,\right)\end{aligned} \tag{8.4}$$

[1] We have dropped the time argument of $\rho_S(t)$.

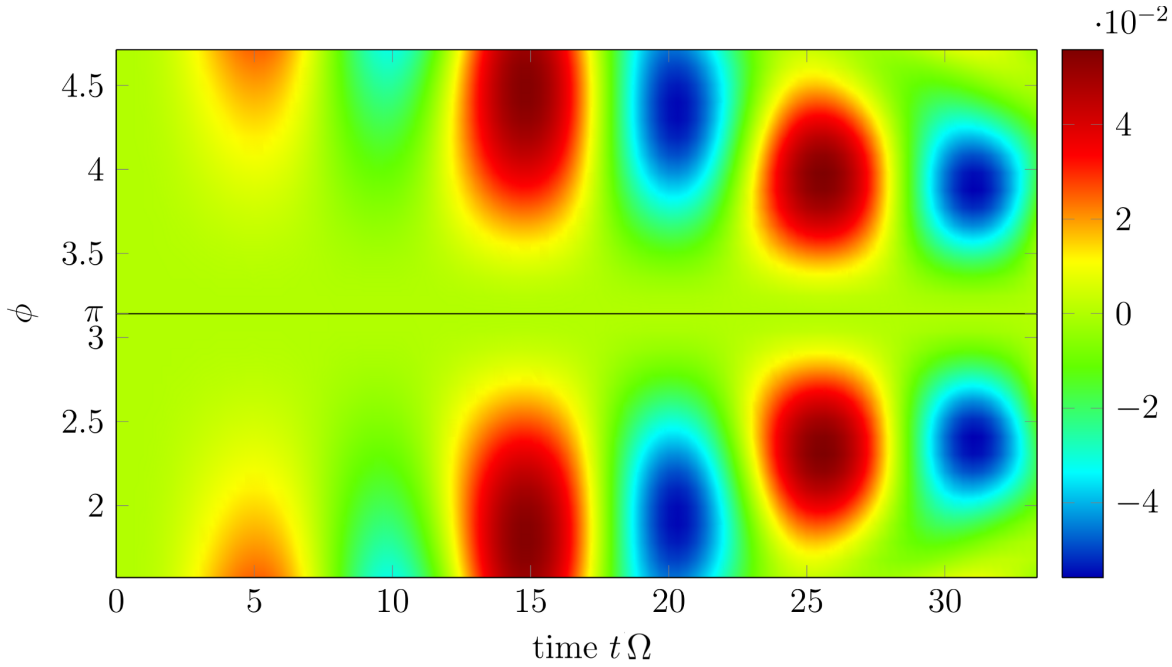

Figure 8.2.: Unitary time evolution of the expectation value of the current (in units of Ω) onto the rightmost level for different magnetic fluxes $\phi \in [\pi/2, 3\pi/2]$. The two levels are degenerate in energy. For $\phi = \pi$ there is no current due to destructive interference.
The parameters used are: $\Omega_1 \equiv \Omega_2 \equiv \Omega_L \equiv \Omega_R = 1\Omega, g = 0.2\Omega$. At time $t = 0$ there is one electron in the left level.

where the dynamics different from the model with just two levels and two baths arises solely from the Hamiltonian H_S. The decay constants are again given by:

$$\gamma_-^{(i)} = \pi J(\Omega_i)(1 - f(\Omega_i, T_i)) \tag{8.5}$$

$$\gamma_+^{(i)} = \pi J(\Omega_i) f(\Omega_i, T_i) \tag{8.6}$$

8.3. Aharanov-Bohm Oscillations

In order to check the phase coherence of the current in the steady state which we obtain from the QME in Lindblad form we again defer to numerical simulations. The rightmost level will now also be populated by its bath. Due to the coupling in the Hamiltonian part of the QME the steady state occupancy of the rightmost level will, however, not only be determined by its bath but also by the current from the other levels which will in turn depend on the acquired phase ϕ. This is, of course, if phase coherence is preserved. If this was not the case we would obtain a current which would be independent of ϕ.

Figures 8.4 and 8.5 show the time evolution of the flux onto (positive) or from (negative) the rightmost level in the steady state in dependence on the phase acquired by coupling from the leftmost to the first level. As expected, the current vanishes completely for a

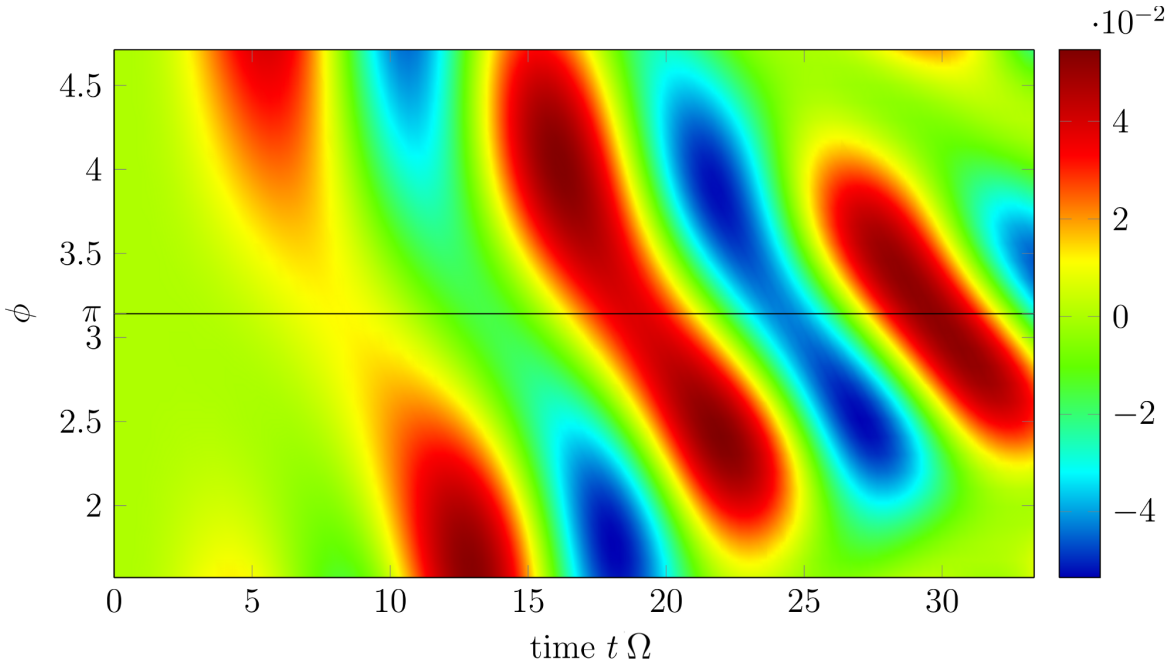

Figure 8.3.: Unitary time evolution of the expectation value of the current (in units of Ω) onto the rightmost level for different magnetic fluxes $\phi \in [\pi/2, 3\pi/2]$. Now the two energy levels are no longer degenerate so that even for $\phi = \pi$ there exists a finite current as the two currents from the first and second level do not cancel exactly anymore. The parameters used are: $\Omega_1 \equiv \Omega_L \equiv \Omega_R = 1\Omega, \Omega_2 = 1.2\Omega, g = 0.2\Omega$. At time $t = 0$ there is one electron in the left level.

phase $\phi = \pi$ and energies $\Omega_1 = \Omega_2$ (see Fig. 8.4) due to destructive interference. For the case $\Omega_1 \neq \Omega_2$ there is only partially destructive interference such that the current does not vanish for $\phi = \pi$.

In conclusion, the QME for the Aharanov-Bohm ring yields phase coherence.

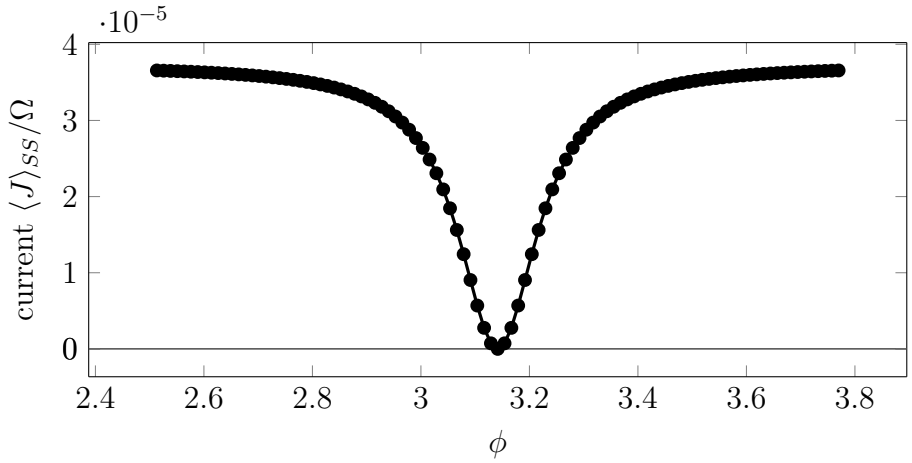

Figure 8.4.: Dependence of the current on the phase angle ϕ for $\Omega_1 = \Omega_2$. For $\phi = \pi$ the steady-state current vanishes.
The parameters used are: $\Omega_1 \equiv \Omega_2 \equiv \Omega_3 \equiv \Omega_4 = 1\Omega, g = 0.2\Omega, V = 0.02\Omega$.

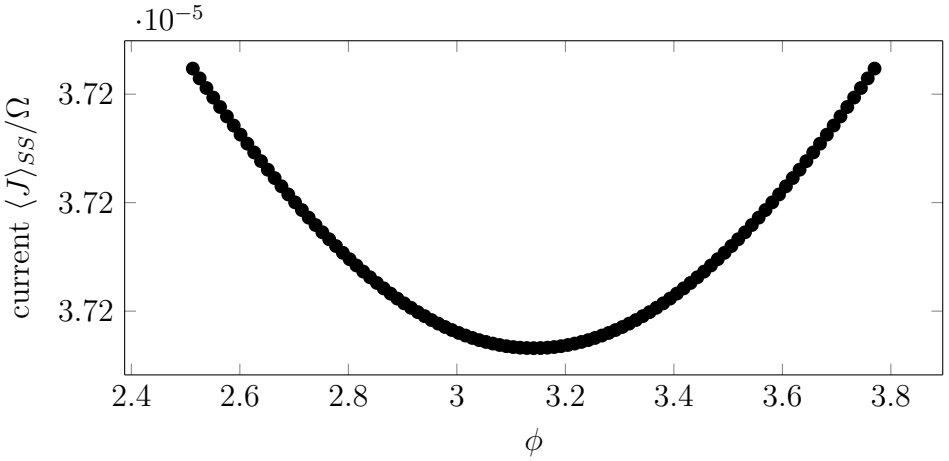

Figure 8.5.: Dependence of the current on the phase angle ϕ for $\Omega_1 \neq \Omega_2$. For $\phi = \pi$ the current is still minimal but clearly non-zero.
The parameters used are: $\Omega_1 \equiv \Omega_3 \equiv \Omega_4 = 1\Omega, \Omega_2 = 1.2\Omega, g = 0.2\Omega, V = 0.02\Omega$.

9. Central Level Coupled to two Explicitly Modeled Leads

In this chapter we consider more complicated systems where there are not one or two lead levels but (ideally) infinitely many. From the last chapters we know how to write down the master equation for the system consisting of two lead levels and we will generalize this to the case of many lead levels. It is our aim to derive properties of the steady state, especially an expression for the particle current through the central level. We hope that for the wide-band limit of a large number of equally spaced lead levels we recover an approximation of the exact result for a single level which is coupled to two leads.

This chapter is organized as follows: After introducing the model we first quote the exact result from the literature. We then state the explicit formula of the QME and determine implicit expressions for the steady state properties of the occupations and the tunneling terms. These are derived similarly to the case with just two levels and two baths (cf. chapter 7). The case of up to 70 lead levels on each side is calculated numerically for the case of equal level spacing in the leads. In the end we compare these results to the exact expression for the current obtained from Keldysh formalism.

The model we consider is the following: A central level of energy Ω is coupled to two leads each consisting of many lead levels q of energy $\omega_{\alpha,q}$ ($\alpha \in \{L, R\}$) via a tunneling term of uniform strength g. Every lead level is in turn coupled to its respective bath of temperature T_α where the coupling strength is described by the (also uniform) parameter V. A generic system is shown in Fig. 9.1. As we want to study the systems numerically we have to limit the number of modeled lead modes $N = N_L + N_R$ and assume them to be equally spaced over their entire bandwidth D such that $\omega_q \in [-D, D]$. For the simple models considered in previous chapters we have used a constant density of states $\rho = 1/\Omega$ (where Ω was an energy scale of the problem) in the level width function Γ. However, we now have to distinguish between the quantities of the baths and the leads. We therefore adopt the following notation summarized in Tab 9.1.

Level spacing in leads	Δ_{lead}	$=$	$2D/N_L$
Density of states in the leads	ρ_{lead}	$=$	$\Delta_{\text{lead}}^{-1}$
Density of states in the baths	ρ_{bath}		
Level width fct. of central level	Γ	$=$	$2\pi g^2 \rho_{\text{lead}}$
Level width fct. of lead levels	Γ_{lead}	$=$	$2\pi V^2 \rho_{\text{bath}}$

Table 9.1.: Notation adopted in this chapter

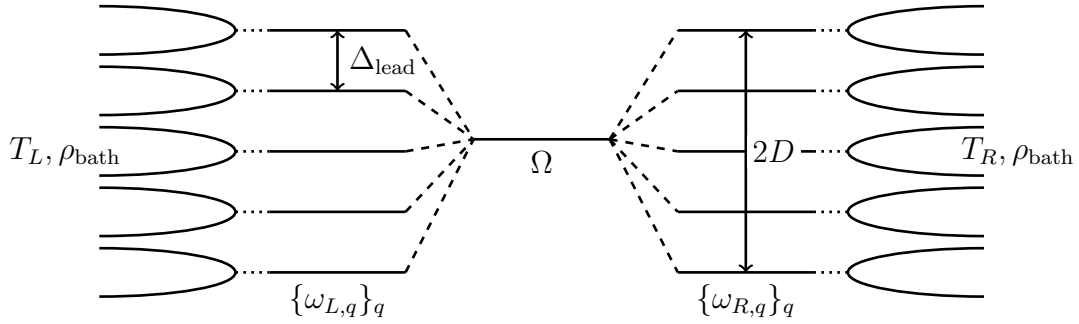

Figure 9.1.: Depiction of the general scheme we consider in this chapter. The central mode is coupled to two leads consisting of many modes q each of which is coupled to its respective bath. All the baths on the left (right) side have the same temperature T_L (T_R).

9.1. Exact Result from Keldysh Formalism

Before we derive an approximate result via a master equation approach we quote the exact result for a single level which is coupled to two leads of temperatures T_L and T_R from [1, Chapt. 12]. The exact result for the particle current with continuous spectral density of the leads is[1]

$$J = \int \frac{d\omega}{2\pi} \frac{\Gamma^L \Gamma^R}{(\omega - \Omega)^2 + (\Gamma/2)^2} (f_L(\omega) - f_R(\omega)) \tag{9.1}$$

where $f_\alpha(\omega)$ are the respective Fermi-Dirac distributions and $\Gamma = \Gamma^L + \Gamma^R$ is the level width function of the central level introduced in Tab. 9.1.

From Eq. (9.1) we see that the difference of the Fermi functions is multiplied by an energy-dependent prefactor which has a Lorentzian shape the width of which is determined by the level width function and therefore by the coupling constant g.

9.2. Master Equation and Steady State Expectation Values

It is straight forward to generalize the QMEs we have obtained in previous chapters to the case of more than two lead levels as in the local approximation there is a separate dissipative contribution for each lead level. The Hamiltonian of the central level and the two leads is given by:

$$H_S = \Omega d^\dagger d + \sum_{\alpha,q} \omega_{\alpha,q} d^\dagger_{\alpha,q} d_{\alpha,q} + \sum_{\alpha,q} \left(g d^\dagger d_{\alpha,q} + \text{h.c.} \right) \tag{9.2}$$

[1]Note that we have changed their notation to ours introduced in Tab. 9.1 and Fig. 9.1.

The QME for the reduced density matrix of the system therefore reads:

$$\frac{d}{dt}\rho_S(t) \equiv \mathcal{L}\rho_S(t) = -i\left[H_S, \rho_S(t)\right] + \sum_{\alpha,q} \mathcal{D}_{\alpha,q}\rho_S(t), \tag{9.3}$$

where the respective dissipators $\mathcal{D}_{\alpha,q}$ are given by the Lindblad terms for the lead level (α, q):

$$\begin{aligned}\mathcal{D}_{\alpha,q}\left[\cdot\right] = \gamma_-(\omega_{\alpha,q}, T_\alpha)\left\{2d_{\alpha,q}[\cdot]d^\dagger_{\alpha,q} - d^\dagger_{\alpha,q}d_{\alpha,q}[\cdot] - [\cdot]d^\dagger_{\alpha,q}d_{\alpha,q}\right\} \\ + \gamma_+(\omega_{\alpha,q}, T_\alpha)\left\{2d^\dagger_{\alpha,q}[\cdot]d_{\alpha,q} - d_{\alpha,q}d^\dagger_{\alpha,q}[\cdot] - [\cdot]d_{\alpha,q}d^\dagger_{\alpha,q}\right\}\end{aligned} \tag{9.4}$$

The decay constants can be expressed in terms of the Fermi functions at the respective energies and temperatures and are given by:

$$\gamma_-(\omega_{\alpha,q}, T_\alpha) = (1 - f_\alpha(\omega_{\alpha,q}))\Gamma_{\text{lead}}/2 \tag{9.5}$$

$$\gamma_+(\omega_{\alpha,q}, T_\alpha) = f_\alpha(\omega_{\alpha,q})\Gamma_{\text{lead}}/2 \tag{9.6}$$

In order to determine the expectation value of an operator in the steady state we use the same method as before, namely calculate its time derivative according to equation (6.25) and set it equal to zero. As the resulting expression will, in general, include expectation values of other operators we will have to calculate their steady state values as well using the same procedure.

The operator describing the particle current from the left lead to the central level can be derived in complete analogy to the Aharanov-Bohm-ring (cf. Eq. (8.3)) and is given by the following expression[2]:

$$J = \frac{g}{i}\sum_q \left(d^\dagger d_{L,q} - d^\dagger_{L,q}d\right) \tag{9.7}$$

For the case of the current operator we therefore have to calculate the expectation values for all possible pairs of creation and annihilation operators. Doing so we arrive at the following coupled equations[3]:

$$\frac{d}{dt}\left\langle d^\dagger d\right\rangle = ig\sum_{\alpha,q}\left(\left\langle d^\dagger_{\alpha,q}d\right\rangle - \left\langle d^\dagger d_{\alpha,q}\right\rangle\right) \tag{9.8}$$

$$\frac{d}{dt}\left\langle d^\dagger_{\alpha,q}d_{\alpha,q}\right\rangle = -2\gamma\left\langle d^\dagger_{\alpha,q}d_{\alpha,q}\right\rangle + ig\left(\left\langle d^\dagger d_{\alpha,q}\right\rangle - \left\langle d^\dagger_{\alpha,q}d\right\rangle\right) + 2\gamma^+_{\alpha,q} \tag{9.9}$$

$$\frac{d}{dt}\left\langle d^\dagger d_{\alpha,q}\right\rangle = -\left[i(\omega_{\alpha,q} - \Omega) + \gamma\right]\left\langle d^\dagger d_{\alpha,q}\right\rangle + ig\left(\sum_{\beta,q'}\left\langle d^\dagger_{\beta,q'}d_{\alpha,q}\right\rangle - \left\langle d^\dagger d\right\rangle\right) \tag{9.10}$$

$$\frac{d}{dt}\left\langle d^\dagger_{\alpha,q}d_{\beta,q'}\right\rangle = -\left[i\left(\omega_{\beta,q'} - \omega_{\alpha,q}\right) + 2\gamma\right]\left\langle d^\dagger_{\alpha,q}d_{\beta,q'}\right\rangle + ig\left(\left\langle d^\dagger d_{\beta,q'}\right\rangle - \left\langle d^\dagger_{\alpha,q}d\right\rangle\right), \tag{9.11}$$

where $\gamma = \gamma_+ + \gamma_- = \frac{\Gamma_{\text{lead}}}{2}$, $\alpha, \beta \in \{L, R\}$ and in the last line we assume $(\beta, q') \neq (\alpha, q)$.

[2]With this choice of sign in the definition of the current operator, positive current flows to the right

[3]Note, that the creation and annihilation operators belonging to different levels anticommute.

In the steady state the time derivatives on the left hand side vanish such that we obtain a system of coupled algebraic equations relating the different steady state expectation values. Due to the constant term in Eq. (9.9) the system of equations is inhomogeneous and we can solve it (and thereby obtain the expectation values) by inverting its coefficient matrix. Note that the size of the coefficient matrix scales as $(N+1)^2 \times (N+1)^2$ where N is the total number of lead modes.

The master equation involves the parameter $\gamma = \frac{\Gamma_{\text{lead}}}{2} = \pi \rho_{\text{bath}} V^2$ determining the coupling strength between the lead mode and its bath. This parameter does not occur in the exact model.

9.3. Exact Treatment of Several Lead Levels

In order to compare the results from the master equation approach to the exact result, we first want to show that they are in agreement with Eq. (9.1). To this ends we keep the Fermi functions as symbolic variables while we numerically perform the inversion of the coefficient matrix which is independent of the temperature. For the case of not too many lead levels (50 to 90 on each side) the coefficient matrix is inverted using `mathematica`. As described above we leave the inhomogeneous part of the equation, i.e. the vector containing the Fermi functions evaluated at the energies of the respective lead modes, as a symbolic expression.

Furthermore, we make the following assumptions regarding the quantities introduced in Tab. 9.1.

- The density of states of the baths is much larger than of the leads: $\rho_{\text{bath}} \gg \rho_{\text{lead}}$. We introduce the ratio $n = \rho_{\text{bath}}/\rho_{\text{lead}} \gg 1$.
- The level width function of the central level should be much larger than the width functions of the leads: $\Gamma \gg \Gamma_{\text{lead}}$
- The level spacing in the leads should be of the order of the level width function of the leads: $\Delta_{\text{lead}} \lesssim \Gamma_{\text{lead}}$

With this we find the following relations:

$$V \gtrsim \frac{1}{\sqrt{2\pi}\rho_{\text{lead}} n} \tag{9.12}$$

$$g \gg Vn \tag{9.13}$$

Due to computational complexity we limit the total number of lead modes to 100.

The particle current in the steady state is obtained by simply plugging in the expectation values for the different terms in Eq. (9.7) obtained by inverting the coefficient matrix . By doing so we arrive at an expression of the form

$$J = \sum_{\alpha,q} C_{\alpha,q} f_{\alpha,q}, \tag{9.14}$$

where $f_{\alpha,q}$ again denotes the Fermi function evaluated for the lead mode (α, q) and $C_{\alpha,q}$ is its coefficient which is independent of the temperature but may still be different for left and right lead.

Via numerical analysis we find that, to very high accuracy, the prefactors of the Fermi functions belonging to the same energy are indeed the same except for a sign. We therefore obtain

$$J = \sum_q C_q (f_{L,q} - f_{R,q}), \tag{9.15}$$

where C_q is now the joint coefficient for the Fermi function of energy ω_q which is independent of the temperature and the index α.

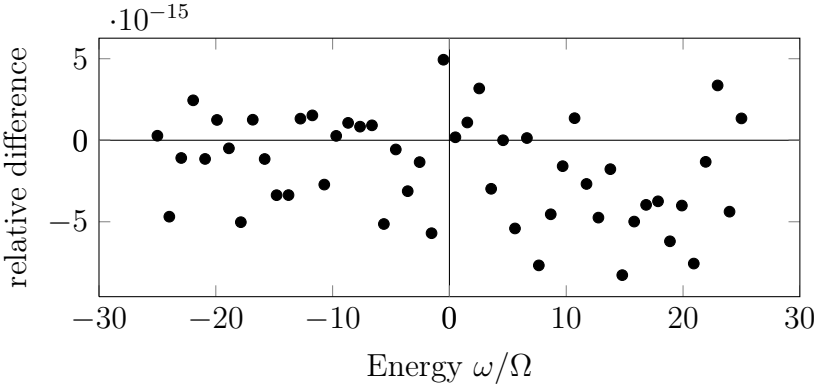

Figure 9.2.: Relative difference between $C_{L,q}$ and $-C_{R,q}$. The extra minus sign comes in as all $C_{R,q}$ are negative whereas all $C_{L,q}$ are positive. The parameters used are $N_{tot} = 100, D = 25\Omega, \Omega = 1, \rho_{\text{bath}} = 10\Omega^{-1}, \rho_{\text{lead}} = 1\Omega^{-1}, \Gamma_{\text{lead}} = 0.2\Omega, \Gamma = 2\pi\Omega$

How good this agreement is can of course be quantified. In Fig. 9.2 we give an example for the distribution of the relative difference. For different parameters we obtain qualitatively the same behavior where the relative difference was always found to be smaller than 10^{-13}. We attribute this difference to numerical errors in the matrix inversion.

With this we can compare our numerical results to the exact formula (9.1). We plot the coefficients C_q in equation (9.15) and obtain a Lorentzian distribution. Due to the limited bandwidth we obtain large errors once the distribution does not fall off to zero fast enough in the tails. This can well be seen in Fig. 9.4 where for the blue and black curves one tail fits well with the exact curve whereas the other one is further off then for the red curve. Furthermore, in Fig. 9.3 the black curve is completely wrong due to these finite size effects. That this problem can indeed be overcome is shown in Fig. 9.5 where we have increased the number of lead levels to 140 (which took about 10 times longer to calculate).

We find that its width depends on g (cf. Fig. 9.3) and is centered around Ω (cf. Fig. 9.4) as is expected from the exact result. We find that for smaller values of the intersubsystem coupling g respectively the level width function Γ the numerical results fit the exact ones better. We partly attribute this to the finite size effects discussed

above. For a specific choice of parameters we give a refined plot with 180 lead levels in Fig. 9.6 which agrees better with the exact curve. However, the peak height does not fit the exact result. This may also be due to the fact that we have neglected the energy shifts of the lead levels due to the coupling to the central level via g (see discussion below Eq. (7.41)). We expect this effect to decrease when increasing the number of levels further.

In conclusion, we find that for the parameter regime considered the QME is in good agreement with the exact results from Keldysh formalism as long as the bandwidth – and therefore the number of lead levels – is chosen large enough.

In order to increase the number of levels beyond 150 it might be useful to introduce an approximation scheme as not all expectation values are equally significant. Especially terms of the form $\langle d^\dagger_{\alpha,q} d_{\beta,q'} \rangle$ with $q \neq q'$ might be good candidates for such an approximation. Performing the matrix inversion with specialized algorithms in `C++` instead of `mathematica` might also yield a speed-up that would allow for a larger number of lead modes.

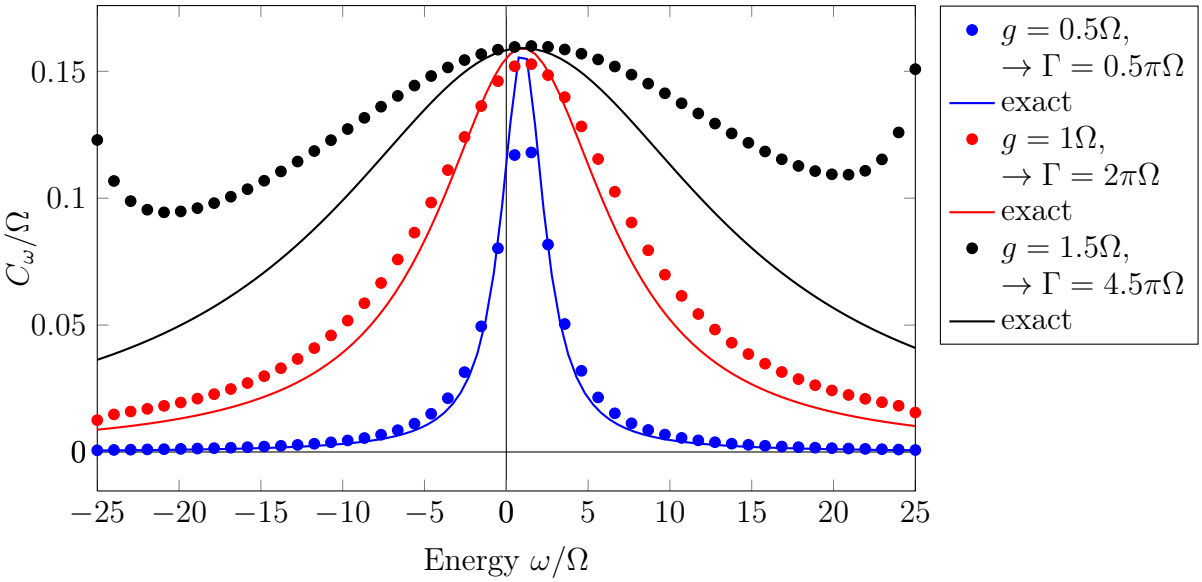

Figure 9.3.: Plot of the coefficient function C_ω for different values of g. The parameters used are $N_{tot} = 100, D = 25\Omega, \Omega = 1, \rho_{\text{bath}} = 10\Omega^{-1}, \rho_{\text{lead}} = 1\Omega^{-1}, \Gamma_{\text{lead}} = 0.2\Omega$. The dots are numerical values whereas the solid lines are exact formulae.

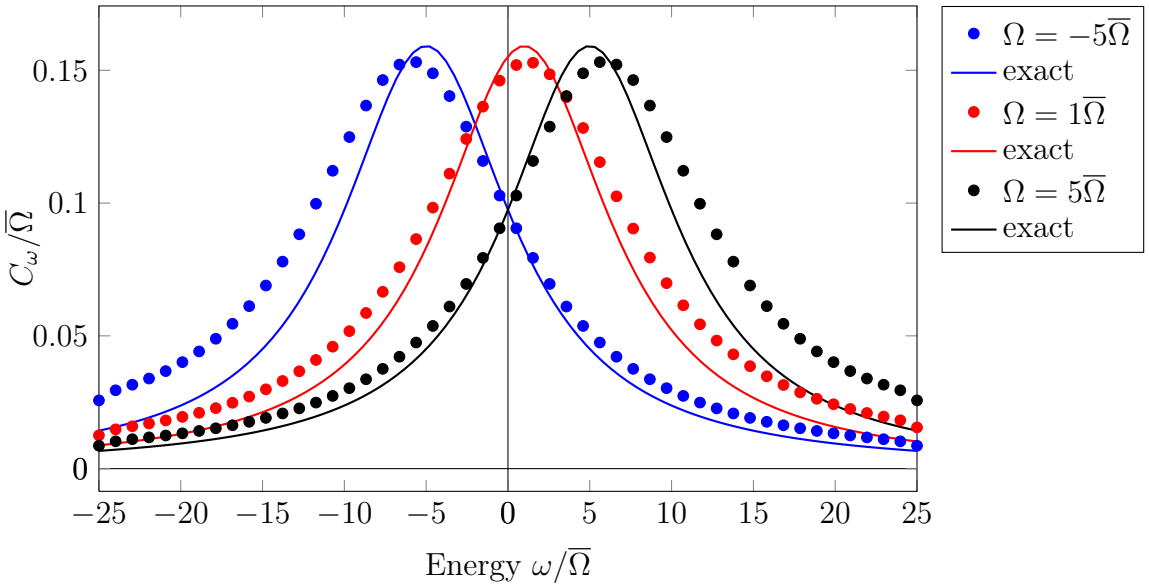

Figure 9.4.: Plot of the coefficient function C_ω for different values of Ω. The parameters used are $N_{tot} = 100, D = 25\overline{\Omega}, \rho_{\text{bath}} = 10\overline{\Omega}^{-1}, \rho_{\text{lead}} = 1\overline{\Omega}^{-1}, \Gamma_{\text{lead}} = 0.2\overline{\Omega}, \Gamma = 2\pi\overline{\Omega}$.

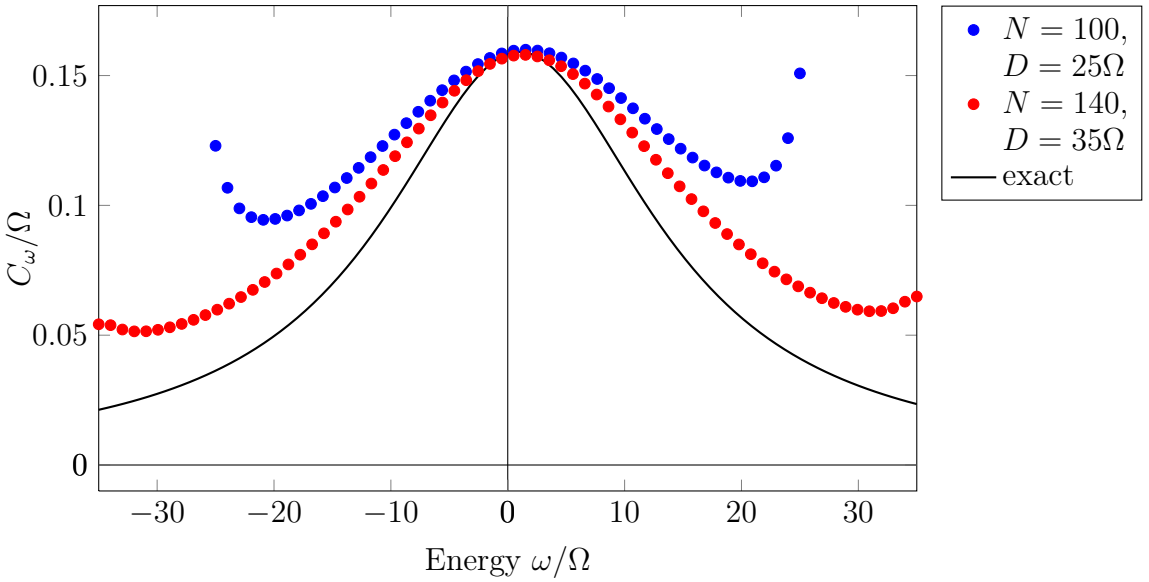

Figure 9.5.: Plot of the coefficient function C_ω for different values of N and D. Due to the limited number of lead modes the simulation produces large errors for too large values of Γ. For an increasing number of lead modes and a larger bandwidth the results improve.
The parameters used are $\rho_{\text{bath}} = 10\Omega^{-1}, \rho_{\text{lead}} = 1\Omega^{-1}, \Omega = 1, \Gamma_{\text{lead}} = 0.2\Omega, \Gamma = 4.5\pi\Omega$.

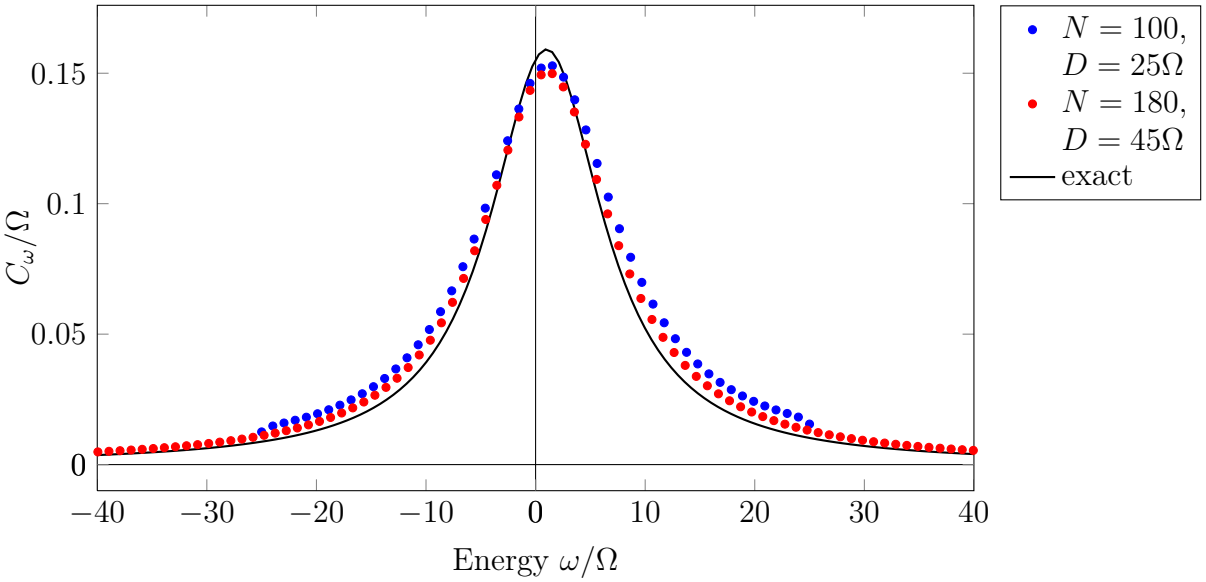

Figure 9.6.: Plot of the coefficient function C_ω for different values of N and D. We see that increasing the number of lead modes slightly improves the results. The parameters used are $\rho_{\text{bath}} = 10\Omega^{-1}, \rho_{\text{lead}} = 1\Omega^{-1}, \Omega = 1, \Gamma_{\text{lead}} = 0.2\Omega, \Gamma = 2\pi\Omega$.

10. Conclusion and Outlook

In this thesis, we have discussed the derivation and steady-state properties of quantum master equations in Lindblad form for different noninteracting fermionic toy-models, both in equilibrium and nonequilibrum. In particular, the transport properties of the considered systems, ranging from two simple resonant levels to two explicitly modeled leads of up to 180 modes, have been investigated and compared to the results obtained from Keldysh formalism which they yield a good agreement to. We were therefore able to provide an explicit consistency check for a Lindblad approach that has potential for describing nonequilibrium steady-state transport in the context of quantum impurity models with local interactions.

We have started by considering the simplest building block of the more complicated systems, the resonant level model, in Chap. 5. Commencing with the Liouville-von Neumann equation in the interaction picture we have applied the Born-Markov approximation in order to arrive at a Lindblad QME for the reduced density matrix of the single level. We have justified the Markov assumption for $\Gamma/T \ll 1$ by explicitly calculating the bath correlation time. We find that the Lindblad bath of temperature T drives the level into its mixed thermal state with respect to the T.

For a composite system of two coupled levels coupled to one or two Lindblad baths, we have found the Born-Markov approximation to be valid when including the intersubsystem coupling in the generator of the interaction picture. We have considered two different approximation schemes in order to arrive at two different QMEs in Lindblad form. In the eigenbasis of the coupled system we derive a QME in the secular approximation which yields, in equilibrium, the correct thermal steady state, whereas it predicts a vanishing particle current for nonequilibrium situations. Therefore, we also have derived a QME in the local basis, by means of neglecting the intersubsystem coupling in the generator of the interaction picture. Due to this the QME lacks the correct description of the steady state in equilibrium. However, introducing a finite temperature gradient, we have obtained a finite current that agrees qualitatively with the exact Keldysh result in a certain parameter regime. We have attributed this to neglecting the intersubsystem coupling in the dissipative terms of the QME.

In Chap. 8 we have used an Aharanov-Bohm like geometry in order to show that the Lindblad QME preserves phase coherence of particle current in the steady state. Introducing a phase shift ϕ for one of the two paths from the left to the right Lindblad bath, we have observed destructive interference of the current for resonant or off-resonant energies of the two paths respectively.

In the last Chap. we have turned to the more complicated system of a single central level coupled to two leads, the levels of which were explicitly modeled, with each coupled to

its respective Lindblad drive. Using a local Lindblad QME we have derived an implicit expression for the expectation value of the particle current operator in the steady state. The expression has numerically been evaluated by means of inverting the coefficient matrix of an inhomogeneous system of algebraic equations, and is found to be in good agreement with the exact Keldysh result for certain parameter regimes.

As has been stressed in Sec. 9.3 the extend to which we have explored this agreement between Lindblad and Keldysh approach is, however, limited as of now. Further possible approaches may include:

- An extension of the number of lead levels for the model which we have considered in Chap. 9. To this end a possible approximation scheme should take into account the fact that not all terms in the above stated system of equations are equally significant.
- The introduction of a second central level, in order to investigate the coherence properties of the particle current by means of Aharanov-Bohm like interference effects similar to those considered in Chap. 8.
- The adoption of yet another approximation scheme for dealing with the QME in the Born-Markov approximation which takes the intersubsystem coupling into account properly. The resulting Lindblad QME would then include the coupling not only in the Hamiltonian part but also in the dissipative terms.

A. Derivations

In this chapter we give the details of derivations and calculations we have omitted in the main part of this thesis.

A.1. Commutation and Anticommutation Relations

As we frequently have to calculate the commutators and anticommutators of products of operators we state here some basic identities which can be verified by simple calculations:

$$[A, BC] = [A, B]\, C + B\, [A, C] \tag{A.1}$$
$$[AB, C] = A\, [B, C] + [A, C]\, B \tag{A.2}$$
$$[A, BC] = \{A, B\}C - B\{A, C\} \tag{A.3}$$
$$[AB, C] = A\{B, C\} - \{A, C\}B \tag{A.4}$$

A.2. Interaction Picture Operators

In this section we derive the interaction picture representation for the creation and annihilation operators frequently used in this thesis.

Let O be an operator in the Schrödinger picture. Then the corresponding operator $\tilde{O}(t)$ in the interaction picture is defined via the equation

$$\tilde{O}(t) = e^{iH_0 t} O e^{-iH_0 t}. \tag{A.5}$$

H_0 is the free Hamiltonian describing the system- and bath-modes. It will in general be given by the following equation:

$$H_0 = \sum_n \Omega_n d_n^\dagger d_n + \sum_{n,k} V_{n,k} c_{n,k}^\dagger c_{n,k} \tag{A.6}$$

where n labels the system-modes and n, k labels the bath-mode k of the nth bath. Note that hybridizing terms can be included into the above Hamiltonian (A.6) by first diagonalizing the system Hamiltonian.

In order to evaluate equation (A.5) we make use of the Baker-Hausdorff formula [12]:

$$\exp(A)B\exp(-A) = B + [A,B] + \frac{1}{2}[A,[A,B]] + \dots \tag{A.7}$$

Upon using the canonical anticommutation-relations for the fermionic creation and annihilation operators we arrive at

$$\begin{aligned}[H_0, d_n] &= \Omega_n \left[d_n^\dagger d_n, d_n\right] \\ &= \Omega_n d_n^\dagger \{d_n, d_n\} - \Omega_n \{d_n^\dagger, d_n\} d_n \\ &= -\Omega_n d_n\end{aligned}$$

which gives rise to the interaction-picture annihilation operator:

$$\tilde{d}_n(t) = e^{-i\Omega_n t} d_n. \tag{A.8}$$

We see that in the interaction picture the annihilation operator merely acquires an additional time-dependent phase. This is due to the fact, that the commutator of d_n with the free Hamiltonian H_0 is again proportional to d_n. This derivation generalizes to all operators that have this property.
We derive the interaction-picture representation of the other operators:

$$\tilde{d}_n(t) = e^{-i\Omega_n t} d_n \tag{A.9}$$

$$\tilde{d}_n^\dagger(t) = e^{i\Omega_n t} d_n^\dagger \tag{A.10}$$

$$\tilde{c}_{n,k}(t) = e^{-i\omega_{n,k} t} c_{n,k} \tag{A.11}$$

$$\tilde{c}_{n,k}^\dagger(t) = e^{i\omega_{n,k} t} c_{n,k}^\dagger \tag{A.12}$$

As we have seen before, the reduced density matrix is obtained by integrating out the degrees of freedom of the environment. This property is conserved when going to the interaction picture.

Proof.

$$\tilde{\rho}_A(t) = \mathrm{tr}_B \tilde{\rho}(t) = \mathrm{tr}_B \left[e^{i(H_A+H_B)t} \rho(t) e^{-i(H_A+H_B)t}\right] \tag{A.13}$$

$$= e^{iH_A t} \mathrm{tr}_B \left[e^{iH_B t} \rho(t) e^{-iH_B t}\right] e^{-iH_A t} \tag{A.14}$$

$$= e^{iH_A t} \mathrm{tr}_B[\rho(t)] e^{-iH_A t} \tag{A.15}$$

$$= e^{iH_A t} \rho_A(t) e^{-iH_A t} \qquad \square$$

Note, that for this proof it is essential that the free Hamiltonian operators commute with each other. This is, however, fulfilled in all the cases we consider as for our models the free Hamiltonians are of second order in the level-operators and the anticommuta-

tors for operators belonging to different levels vanish:

$$\left[d_1^\dagger d_1, c_q^\dagger c_q\right] = d_1^\dagger \left[d_1, c_q^\dagger c_q\right] + \left[d_1^\dagger, c_q^\dagger c_q\right] d_1 \tag{A.16}$$

$$= d_1^\dagger \{d_1, c_q^\dagger\} c_q - d_1^\dagger c_q^\dagger \{d_1, c_q\} + \cdots \tag{A.17}$$

$$= 0 \tag{A.18}$$

A.3. Density Matrix in the Interaction Picture

In Tab. 2.1 we quoted the relation between the density matrix in the Schrödinger and the interaction picture to be:

$$\tilde{\rho}(t) = U_0^\dagger(t, t_0)\rho_S(t)U_0(t, t_0)$$

From that we arrive at:

$$\dot{\tilde{\rho}}(t) = \frac{d}{dt}\left[U_0^\dagger(t, t_0)\rho_S(t)U_0(t, t_0)\right] \tag{A.19}$$

$$= \frac{i}{\hbar}\left[H_0, U_0^\dagger(t, t_0)\rho_S(t)U_0(t, t_0)\right] + U_0^\dagger(t, t_0)\dot{\rho}_S(t)U_0(t, t_0) \tag{A.20}$$

$$= \frac{i}{\hbar} U_0^\dagger(t, t_0)\left[H_0, \rho_S(t)\right] U_0(t, t_0) + U_0^\dagger(t, t_0)\dot{\rho}_S(t)U_0(t, t_0) \tag{A.21}$$

This is equivalent to:

$$\dot{\rho}_S(t) = -\frac{i}{\hbar}\left[H_0, \rho_S(t)\right] + U_0(t, t_0)\dot{\tilde{\rho}}(t)U_0^\dagger(t, t_0) \tag{A.22}$$

$$= -\frac{i}{\hbar}\left[H, \rho_S(t)\right] + U_0(t, t_0)\mathcal{D}\tilde{\rho}(t)U_0^\dagger(t, t_0), \tag{A.23}$$

where $\mathcal{D}$ is the dissipative part (i.e. Lindblad-operators) of the master equation.

A.4. Alternate Derivation of QME in Born-Approximation

In this section we give an alternate derivation of the QME in the Born-approximation. We will very closely follow [4]. We again start from the Liouville-von Neumann equation in the interaction picture

$$\frac{d}{dt}\tilde{\rho} = -i\left[\tilde{H}_I(t), \tilde{\rho}(t)\right]$$

which we can integrate formally in the case that the coupling is not explicitly time-dependent:

$$\tilde{\rho}(t) = \rho(t_0) - i\int_{t_0}^{t} dt' \left[\tilde{H}_I(t'), \tilde{\rho}(t')\right]$$

We now plug this result into the right hand side of the Liouville-von Neumann equation and obtain:

$$\frac{d}{dt}\tilde{\rho}(t) = -i\left[\tilde{H}_I(t), \tilde{\rho}(t_0)\right] - \int_{t_0}^{t} dt' \left[\tilde{H}_I(t), \left[\tilde{H}_I(t'), \tilde{\rho}(t')\right]\right] \tag{A.24}$$

In order to arrive at an equation for the reduced density matrix we trace over the degrees of freedom of the environment and again invoke the factoring assumption of the density matrix at an initial time t_0: $\tilde{\rho}(t_0) = \tilde{\rho}_S(t_0) \otimes \rho_0$. Note, however, that we now also have to assume that this factorization will prevail for later times $t > t_0$. In the literature (cf. for example [4]) it is argued that this is approximately the case for weak couplings and for the case that the environment is so large that it does not change due to the coupling to the system. This then yields:

$$\frac{d}{dt}\tilde{\rho}_S(t) = -i\mathrm{tr}_B\left[\tilde{H}_I(t), \tilde{\rho}_S(t_0)\otimes\rho_0\right] - \int_{t_0}^{t} dt' \mathrm{tr}_B\left[\tilde{H}_I(t), \left[\tilde{H}_I(t'), \tilde{\rho}_S(t')\otimes\rho_0\right]\right], \tag{A.25}$$

which simplifies for the case of a thermal bath[1] and after changing the integration variable to the equation we obtained above using projection operator methods:

$$\frac{d}{dt}\tilde{\rho}_S(t) = -\int_{0}^{t} ds \mathrm{tr}_B\left[\tilde{H}_I(t), \left[\tilde{H}_I(t-s), \rho(t-s)\otimes\rho_0\right]\right] \tag{A.26}$$

As we have noted before, the assumption that the factorization of system and bath prevails is an effective second order approximation in the coupling strength to the bath.

A.5. Bath Correlation Function

In order to calculate the integral in Eq. (4.28) we make use of the residue theorem (see for example [12])

$$\oint_C f(z)dz = 2\pi i \sum_{z_0} \mathrm{Res}(f(z), z_0) \tag{A.27}$$

Where the sum runs over all roots z_0 of $f(z)$ in the complex plane enclosed by the contour C and $\mathrm{Res}(f(z), z_0)$ denotes the residue of $f(z)$ at z_0.
For a pole of first order the residue is given by:

$$\mathrm{Res}(f(z), z_0) = \lim_{z\to z_0}(z - z_0)f(z) \tag{A.28}$$

For the above integral we choose the contour to describe a semicircle in the upper half-plane. The function $f(z)$ is in our case given by

$$f(z) = \frac{e^{izt}}{e^{cz}+1}$$

[1] $\mathrm{tr}_B(\tilde{H}_I(t)\tilde{\rho}_S(t)\otimes\rho_0) = 0$. This is equivalent to eq. (4.15)

whose complex roots in the upper half plane are $z_{0_n} = \frac{i\pi}{c}(2n+1), n \in \mathbb{N}_0$. Expanding the exponential in the denominator and factoring out the complex root yields:

$$f(z) = -\frac{1}{z - \frac{i\pi}{c}(2n+1)} \frac{e^{izt}}{c + \frac{1}{2!}c^2(z - \frac{i\pi}{c}(2n+1)) + \cdots} \tag{A.29}$$

Thus with use of formula (A.28) we calculate the residue:

$$\begin{aligned}
\mathrm{Res}\left(\frac{e^{i\omega t}}{e^{c\omega}+1}, \frac{i\pi}{c}(2n+1)\right) &= \lim_{z \to i\pi/c(2n+1)} (z - \frac{i\pi}{c}(2n+1)) \frac{e^{i\omega t}}{e^{c\omega}+1} && \text{(A.30)} \\
&= \lim_{z \to i\pi/c(2n+1)} -\frac{e^{i\omega t}}{c + \frac{1}{2!}c^2(z - \frac{i\pi}{c}(2n+1)) + \cdots} && \text{(A.31)} \\
&= -\frac{1}{c} e^{-\frac{\pi}{c}(2n+1)t} && \text{(A.32)}
\end{aligned}$$

and obtain for the bath correlation function

$$\begin{aligned}
C(\tau) &= \rho \int_{-\infty}^{\infty} d\omega \frac{e^{i\omega\tau}}{e^{\omega/T}+1} && \text{(A.33)} \\
&= 2\pi i \rho \sum_{n \geq 0} \mathrm{Res}\left(\frac{e^{i\omega\tau}}{e^{\omega/T}+1}, i\pi T(2n+1)\right) && \text{(A.34)} \\
&= 2\pi i \rho T \sum_{n \geq 0} e^{-\pi T(2n+1)\tau} && \text{(A.35)} \\
&= 2\pi i \rho T e^{-\pi T\tau} \frac{1}{1 - e^{-2\pi T\tau}} && \text{(A.36)} \\
&= -i\pi\rho T \frac{1}{\sinh(\pi T\tau)} && \text{(A.37)}
\end{aligned}$$

A.6. Born-Markov Approximation

We give a short derivation of Eq. (4.32)

$$\begin{aligned}
\frac{d}{dt}\tilde{\rho}_S(t) &= -\int_0^{\infty} ds \mathrm{tr}_B \left[\tilde{H}_I(t), \left[\tilde{H}_I(t-s), \rho(t) \otimes \rho_0\right]\right] && \text{(A.38)} \\
&= -\int_0^{\infty} ds \mathrm{tr}_B \Big\{\tilde{H}_I(t)\tilde{H}_I(t-s)\tilde{\rho}_S(t)\rho_0 - \tilde{H}_I(t)\tilde{\rho}_S(t)\rho_0\tilde{H}_I(t-s) && \text{(A.39)} \\
&\qquad - \tilde{H}_I(t-s)\tilde{\rho}_S(t)\rho_0\tilde{H}_I(t) + \tilde{\rho}_S(t)\rho_0\tilde{H}_I(t-s)\tilde{H}_I(t)\Big\} && \text{(A.40)} \\
&= -\int_0^{\infty} ds \mathrm{tr}_B \Big\{\tilde{H}_I(t)\tilde{H}_I(t-s)\tilde{\rho}_S(t)\rho_0 - \tilde{H}_I(t-s)\tilde{\rho}_S(t)\rho_0\tilde{H}_I(t) + \mathrm{h.c.}\Big\} && \text{(A.41)}
\end{aligned}$$

A.7. Diagonalization of two Coupled Levels

In this section we diagonalize the closed quantum system consisting of two levels of different energies Ω_1 and Ω_2 coupled to each other with coupling strength g (see Fig. A.1). We then introduce new creation and annihilation operators in the eigenbasis and express them in terms of the old operators.

The system Hamiltonian H_S can be written as a quadratic form as follows:

$$H_S = \begin{pmatrix} d_1^\dagger & d_2^\dagger \end{pmatrix} \begin{pmatrix} \Omega_1 & g \\ g & \Omega_2 \end{pmatrix} \begin{pmatrix} d_1 & d_2 \end{pmatrix} \tag{A.42}$$

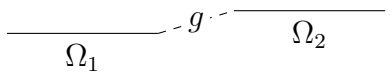

Figure A.1.: Schematic depiction of two levels coupled to each other with coupling strength g.

Straightforward diagonalization gives rise to the two eigenvalues of the above matrix:

$$\Omega_\pm = \frac{\Omega_1 + \Omega_2}{2} \pm \sqrt{g^2 + \left(\frac{\Omega_1 - \Omega_2}{2}\right)^2} \tag{A.43}$$

The new creation and annihilation operators of the combined subsystems are denoted by $D_\pm^\dagger$ and $D_\pm$ respectively and are assumed to be eigenoperators of H_S:

$$\left[H_S, D_\pm^\dagger\right] = \Omega_\pm D_\pm^\dagger \tag{A.44}$$

Furthermore by imposing the normalization condition

$$\langle \pm | \pm \rangle = \langle 0 | D_\pm D_\pm^\dagger | 0 \rangle = 1 \tag{A.45}$$

we can finally express these new operators in terms of those of the subsystems:

$$\begin{pmatrix} D_+^\dagger \\ D_-^\dagger \end{pmatrix} = \underbrace{\begin{pmatrix} \frac{1}{\sqrt{1+\eta_+^2}} & \frac{\eta_+}{\sqrt{1+\eta_+^2}} \\ \frac{1}{\sqrt{1+\eta_-^2}} & \frac{\eta_-}{\sqrt{1+\eta_-^2}} \end{pmatrix}}_{=:\,A} \begin{pmatrix} d_1^\dagger \\ d_2^\dagger \end{pmatrix} \tag{A.46}$$

where

$$\eta_\pm = \frac{\Omega_2 - \Omega_1}{2g} \pm \sqrt{1 + \left(\frac{\Omega_2 - \Omega_1}{2g}\right)^2} \tag{A.47}$$

As can easily be checked, the above matrix (A.46) is unitary with real entries. It will hereafter be denoted by A_{ij}. Note that in this new coupled basis, the system Hamiltonian (including the intersubsystem-coupling) is diagonal and can be written as

follows:

$$H_S = \sum_{n=\pm} \Omega_n D_n^\dagger D_n \tag{A.48}$$

Moreover, as the matrix A is unitary, its inverse is given by its hermitian conjugate (here: transpose, as A is chosen to have real entries), such that the creation and annihilation operators of the uncoupled basis are given by:

$$d_i^\dagger = \sum_n (A^{-1})_{in} D_n^\dagger = \sum_n (A^\dagger)_{in} D_n^\dagger = \sum_n A_{ni}^* D_n^\dagger \tag{A.49}$$

A.8. Derivation of the Current Operator

A.8.1. Two Coupled Levels

We give a short derivation of the operator describing the current between two coupled levels. For this we calculate the time derivative of the occupation number operator with respect to the Hamiltonian dynamics using the Heisenberg equation of motion (cf. table 2.1). The Hamiltonian is given by

$$H_S = \Omega_1 d_1^\dagger d_1 + \Omega_2 d_2^\dagger d_2 + g\left(d_1^\dagger d_2 + d_2^\dagger d_1\right), \tag{A.50}$$

which gives rise to the current between the two levels[2]:

$$\frac{d}{dt} N_1 = i\left[H_S, N_1\right] \tag{A.51}$$

$$= \frac{g}{i}\left(d_2^\dagger d_1 - d_1^\dagger d_2\right) \tag{A.52}$$

A.8.2. Aharanov-Bohm like Problems

For the case of the Aharanov-Bohm like system the Hamiltonian dynamics is similar to the case of two coupled levels. The current-operator can be calculated analogously using the Heisenberg equation. Again we only include the Hamiltonian dynamics in the calculation, i.e. the particle current from or to the first and second level[3]. For the Hamiltonian

$$H_S = \sum_{j=1,2,L,R} \Omega_j d_j^\dagger d_j + \left[g\left(e^{i\phi} d_L^\dagger d_1 + d_L^\dagger d_2 + d_R^\dagger d_1 + d_R^\dagger d_2\right) + \text{h.c.}\right] \tag{A.53}$$

[2] sign-convention: positive current flows towards the right

[3] for the nomenclature of the levels refer to the description at the beginning of chapter 8.

the Heisenberg equation yields:

$$\begin{aligned} \frac{d}{dt} N_R &= i \left[H_S, N_R \right] \\ &= \frac{g}{i} \left(d_R^\dagger d_1 - d_1^\dagger d_R + d_R^\dagger d_2 - d_2^\dagger d_R \right) \end{aligned} \tag{A.54}$$

This, again, gives the net particle current onto the rightmost level. The current due to the coupling to the bath-modes is not accounted for by this current operator.

B. Numerics

In this chapter we account for how the numerical results of this thesis have been obtained.

The calculations have been done employing `matlab` and making use of some predefined functions from the Quantum Optics Toolbox for matlab that has been written by Sze Meng Tan from Auckland University [13]. The current version can be found on `http://qwiki.stanford.edu/index.php/Quantum_Optics_Toolbox`.

Further calculations (mostly matrix inversions and symbolic calculations) have been performed using `mathematica`.

B.1. Quantum Optics Toolbox

The Quantum Optics Toolbox comes equipped with a series of classes and functions that make it easy to implement quantum mechanical operators and equations and to, for example, integrate the equations of motion of density matrices. A detailed description of the capabilities and their implementations can be found in the manual.

When implementing the operators for the different fermionic levels one has to define the state $|1 \cdots 1\rangle$ by stating the order in which the fermions are put into their respective level. This fixes the explicit form of the operators which have to fulfill the stated anticommutation relations (cf. section 2.3).

The implementation of superoperators such as the Liouvillian (cf. eq. (2.10)) or the Lindbladian are particularly easy as the toolbox internally treats an $N \times N$ density matrix as a column vector of length N^2 and superoperators as matrices of size $N^2 \times N^2$. Using the built-in commands `spre(M)` and `spost(M)` meaning pre- and postmultiplication with a matrix M the Lindblad quantum master equation is easily implemented. For further details on how this is done internally and in practice refer to the manual.

Expectation values of an operator O in the state $\rho(t)$ can be calculated using the command `expect(O,rho(t))`.

B.2. Calculation of the Steady State

After a quantum master equation is implemented we want to calculate its steady state. There exists a built-in function `steady(L)` that solves the equation

$$\mathcal{L}\rho_{SS} = 0 \tag{B.1}$$

for ρ_{SS}. The algorithm is explained in the manual. For simple superoperators this equation can be solved by calculating its kernel (or nullspace).

B.3. Time-evolution of the Density Matrix, Integration of the Master Equation

The Quantum Optics Toolbox can also integrate the equations of motion of a density matrix

$$\frac{d}{dt}\rho(t) = \mathcal{L}\rho(t) \tag{B.2}$$

with boundary condition $\rho(t = 0) = \rho_0$. The command to achieve this is called `rhoES=ode2es(L,rho0)` and calculates the time-evolution for the eigenvectors of $\mathcal{L}$ and the expansion of rho_0 in this basis. It returns a matrix exponential series that expects a time-argument in order to calculate $\rho(t)$. This evaluation at time t is performed using the command `esval(rhoES,t)`.

Bibliography

[1] H. Haug and A.-P. Jauho. *Quantum Kinetics in Transport and Optics of Semiconductors*. Springer, 2nd rev. ed. edition, 2008. ISBN 3540616020.

[2] I. Weymann, A. Weichselbaum, and J. von Delft. unpublished.

[3] J. J. Sakurai. *Modern Quantum Mechanics (Revised Edition)*. Addison Wesley, rev sub edition, 1993. ISBN 0201539292.

[4] H.-P. Breuer and F. Petruccione. *The Theory of Open Quantum Systems*. Oxford University Press, USA, 2007. ISBN 0199213909.

[5] Á. Rivas and S. F. Huelga. Introduction to the time evolution of open quantum systems. *ArXiv e-prints*, April 2011.

[6] T. Brandes. Chapter 7 (quantum dissipation), lectures on background to quantum information. `http://wwwitp.physik.tu-berlin.de/brandes/public_html/publications/notes.pdf`, 2004.

[7] Á. Rivas, A. D. K. Plato, S. F. Huelga, and M. B. Plenio. Markovian master equations: a critical study. *New Journal of Physics*, 12(11):113032, November 2010. doi: 10.1088/1367-2630/12/11/113032.

[8] Nakatani, M. and Ogawa, T. Quantum Master Equations for Composite Systems: Is Born-Markov Approximation Really Valid? *Journal of the Physical Society of Japan*, 79(8):084401–+, August 2010. doi: 10.1143/JPSJ.79.084401.

[9] H. Carmichael. *Statistical Methods in Quantum Optics 1: Master Equations and Fokker-Planck Equations*. Springer Science+Business Media, 2002.

[10] H. Wichterich, M. J. Henrich, H.-P. Breuer, J. Gemmer, and M. Michel. Modeling heat transport through completely positive maps. *Phys. Rev. E*, 76,:031115, 2007. doi: 10.1140/epjst/e2007-00367-4.

[11] Y. Aharonov and D. Bohm. Significance of electromagnetic potentials in the quantum theory. *Phys. Rev.*, 115(3):485–491, Aug 1959. doi: 10.1103/PhysRev.115.485.

[12] G. B. Arfken and H.-J. Weber. *Mathematical Methods for Physicists*. Academic Press, Fourth (International) edition, 1995. ISBN 0-12-059816-7.

[13] S. M. Tan. Quantum optics toolbox. `http://qwiki.stanford.edu/images/1/1c/Qousersguide.pdf`, 2002.

Acknowledgements

I wish to express my gratitude to my supervisor Prof. Jan von Delft who encouraged me to work on this fascinating topic and supported me whenever I needed help. I would like to thank Prof. von Delft for the many instructive discussions that provided a valuable source of new ideas, and the possibility of doing my Bachelor thesis in his group.

Furthermore, I would like to thank Alexander Dobrinevski for the discussions on many aspects of this work and for proofreading this manuscript.

I also wish to thank several academic sponsorship organizations, most notably the Maximilianeum foundation and the Studienstiftung for financial and non-material support during the entire time of my studies.

Erklärung

Hiermit erkläre ich, dass ich vorgelegte Arbeit selbstständig angefertigt und keine anderen als die angegebenen Quellen und Hilfsmittel verwendet habe.

München, den 26.07.2011 _____

Bauer, Matthias